Cities 174 (2026) 107068

Contents lists available at ScienceDirect

Cities

journal homepage: www.elsevier.com/locate/cities

Explainable second-dimension spatial association between park sentiment and built-social environments

Xiaojun Wang [a,1], Yilong Wu [b,1], Tingyu Shi [a], Rongyu Zhang [c], Yanxi Chen [a], Yongze Song [b,*]

[a] School of Geographical Sciences, Fujian Normal University, Fuzhou, 350117, China
[b] School of Design and the Built Environment, Curtin University, Perth, WA, 6102, Australia
[c] School of Software Engineering, Xiamen University of Technology, Xiamen, 361024, China

ARTICLE INFO

Keywords:
Urban parks
Spatially nonlinear function
Sentiment analysis
Volunteered geographic information

ABSTRACT

Understanding human–environment interactions is crucial for sustainable urban development and well-being. Urban parks are key urban environments affecting residential emotions. However, existing studies with fixed neighborhood ranges and mean-based indicators limit the examination of nonlinear effects across spatial scales and value ranges. This study develops an explainable second dimension of spatial association (ESDA) model to identify spatially nonlinear drivers of park sentiment. The sentiment is quantified using a RoBERTa model with volunteered geographic information for parks in Xiamen, China. ESDA constructs second dimension variables by searching ranges (b) and probability parameters (τ), and fits an SDA-based random forest with SHapley Additive exPlanations (SHAP) for interpretation. Leave-one-out cross-validation shows that SDA ($R^2 = 0.459$) improved modeling accuracy compared with the fixed-neighborhood, mean-based baseline ($R^2 = 0.357$). SHAP indicates nonlinear, scale-dependent, and sign-reversing effects on sentiment. For instance, high near-neighborhood road density and baseline population are associated with lower sentiment, whereas street-scale service aggregation is associated with higher sentiment, and the effects of building height and nighttime light vary with scale and background conditions. The findings suggest prioritizing parks in macro-scale areas with high accessibility and activity levels, while avoiding parcels with overly dense nearby roads and high existing light levels or population. In conclusion, the spatial nonlinearity is diagnosed through the ESDA model that constructs critical b–τ combinations and integrates SHAP for layered park siting and surrounding-environment optimization.

1. Introduction

The sixth UN Global Environment Outlook (GEO-6) emphasizes that transforming human-environment interactions is crucial for addressing global sustainability challenges (UNEP, 2019). These interactions are manifested not only in material resource use, but also in human perceptions of the environment (Liu et al., 2007). As urbanization accelerates, urban green spaces such as parks become vital arenas where these interactions unfold at a micro scale (Kabisch et al., 2015). Parks shape visitors' emotional experiences and environmental perceptions by providing both ecosystem services and spaces for social engagement (Huai & Van de Voorde, 2022; Kong et al., 2022). In this context, analyzing sentiment toward urban parks can provide valuable insights into the evolving human–environment relationship within rapidly changing urban landscapes.

Determining the drivers of visitor sentiment and satisfaction is critical to urban park research. The primary drivers examined in the existing studies include physical facilities and landscape features within parks. Investigations utilizing questionnaire surveys or social media text mining to extract perceptual dimensions have confirmed the notable positive effects of high-quality internal attributes on visitor experiences (Grahn & Stigsdotter, 2010; Huai & Van de Voorde, 2022; Ma & Jiang, 2023). However, internal quality is limited in fully explaining variances in visitor sentiment (Li et al., 2023; Liu et al., 2023; Zhao et al., 2025). Surrounding environmental factors, such as accessibility and economic vitality, are equally critical to visitor sentiment and satisfaction. These external attributes mainly operate by shaping access burdens and travel experiences, while also modulating perceived safety and environmental stress (Ghahramani et al., 2021; Li et al., 2023, 2025; Zhao et al., 2025).

Existing studies on factors influencing park sentiment largely rely on

* Corresponding author.
E-mail address: yongze.song@curtin.edu.au (Y. Song).
[1] These authors contributed equally to this work.

https://doi.org/10.1016/j.cities.2026.107068
Received 3 June 2025; Received in revised form 16 February 2026; Accepted 30 March 2026
Available online 11 April 2026

traditional linear regression and conventional machine learning techniques. Linear regression is widely used for its transparency and interpretability (Huai & Van de Voorde, 2022; Liang et al., 2022). However, its inherent linear assumptions limit its capacity to model complex nonlinear relationships, and it requires manual specification to account for interaction effects (Hastie & Tibshirani, 1986). To address these constraints, recent studies have adopted machine-learning algorithms such as random forests (Kong et al., 2022; Lai et al., 2023). Their nonparametric structure and recursive partitioning can capture nonlinear relationships and high-order interactions without requiring explicit functional-form specification. However, black-box models lack explicit mechanisms for characterizing spatial heterogeneity. To address these limitations, researchers have adopted spatial statistical methods such as Geodetector (Wang & Xu, 2017) and MGWR (Fotheringham et al., 2017) to uncover the spatial variation mechanisms by which environmental factors drive park sentiment or user responses (Fan et al., 2021; Zhao et al., 2025).

Gaps remain in understanding urban park sentiment. First, prior studies prioritized internal park attributes, such as physical facilities and landscape features, over the surrounding environment (Li et al., 2023; Zhao et al., 2025). Second, characterizations of the park periphery often rely on a single, fixed neighborhood (Kong et al., 2022; Li et al., 2023). However, the Uncertain Geographic Context Problem (UGCoP) suggests that estimates of contextual effects may be sensitive to neighborhood delineation and scale specification, because the true spatial extent of the relevant geographic context is often not clearly defined (Kwan, 2012). This motivates examining multi-scale effects of urban environmental variables and testing whether effect directions reverse under scale transformation (Farkas et al., 2023; Hong et al., 2014). Third, most studies simplify spatial features by aggregating data with single statistics, such as the mean (Li et al., 2023; Zhang & Tan, 2019; Zhao et al., 2025). Even where multi-scale perspectives are attempted (Zhang & Tan, 2019), the reliance on simple averages reflects "Gaussian thinking" that overlooks non-linear effects arising from fine-grained differences in factor attribute values (Jiang, 2015). Fourth, although machine learning models have been increasingly adopted, they seldom uncover how the direction and strength of factor effects vary across value ranges (Teng et al., 2024; Zhang et al., 2023). However, real-world geographic processes frequently exhibit environmental variable effects that are non-monotonic across both scale and value dimensions (Holland & Yang, 2016; Zhang et al., 2015). Together, the prioritization of internal park attributes over surrounding environments, fixed single-neighborhood characterization, simple averaging, and black-box modeling paradigms make it difficult for existing research to capture and explain the complex spatial pattern of relationships between park visitor sentiment and surrounding environments.

This study defines park sentiment as a spatially nonlinear function of surrounding environmental variables, capturing spatially non-stationary responses arising from the interaction between value differences and scale transformations. To systematically integrate these two non-linear effects of the urban park periphery, we introduce the Second Dimension of Spatial Association (SDA) method (Song, 2022). The Explainable Second Dimension of Spatial Association (ESDA) model is constructed and implemented in urban parks in Xiamen, China, which includes three steps (Fig. 1). The first step is the construction of second dimension variables by searching spatial ranges and probability parameters of environmental factors. The second step is the modeling of park sentiment using an SDA-based random forest (SDA-RF) (Breiman, 2001). The third step is employing Shapley Additive Explanations (SHAP) to characterize the direction and intensity of environmental variable

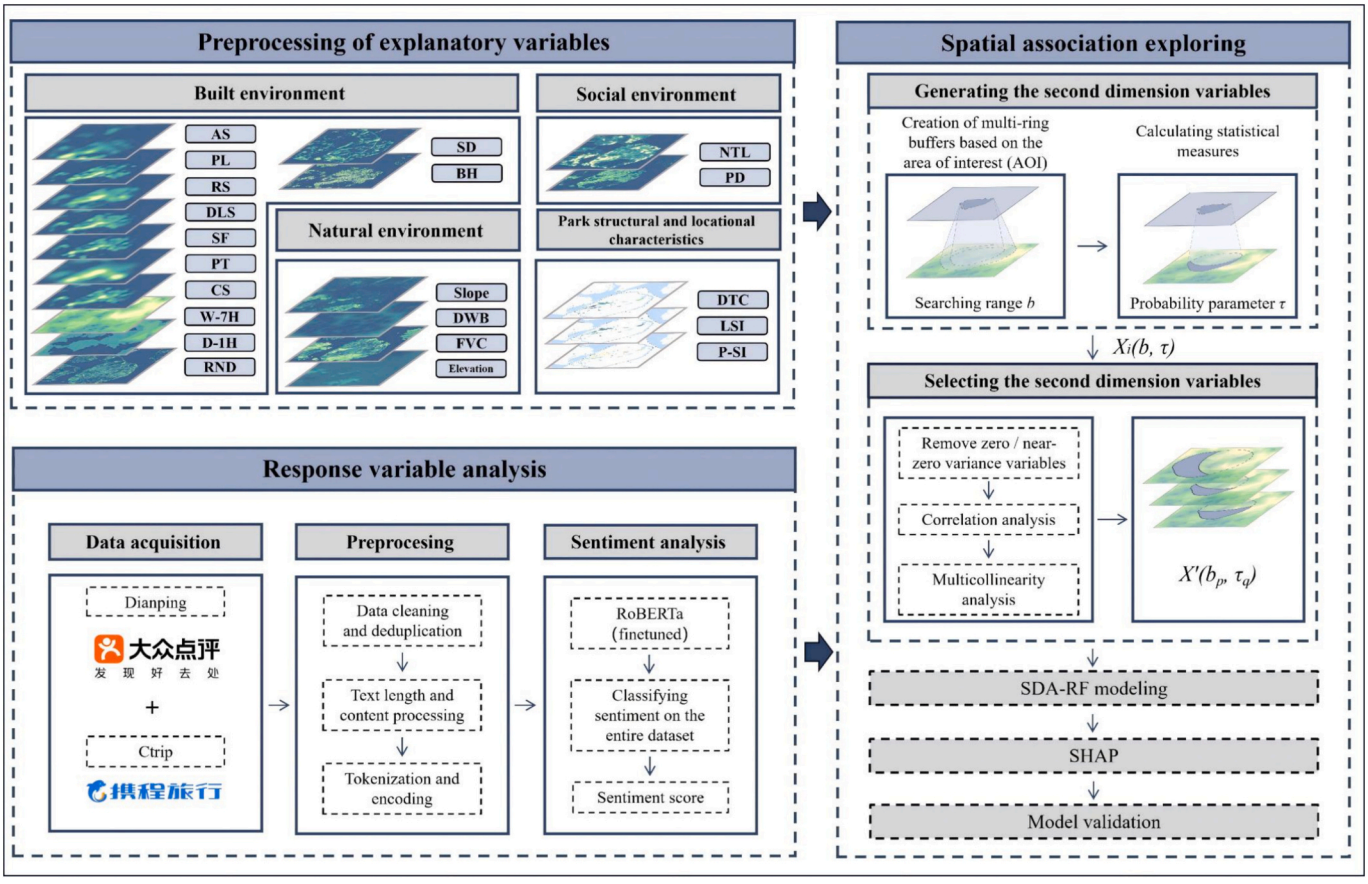

Fig. 1. Flowchart of the ESDA model for diagnosing spatially nonlinear drivers of park sentiment, illustrating stages including preprocessing of explanatory variables, response variable analysis, spatial association exploration using SDA-RF, and SHAP-based interpretation.

contributions (Lundberg & Lee, 2017). This study aims to quantify spatially nonlinear associations between surrounding environments and park sentiment across scales and value segments, determine the most influential factors under specific scale-quantile combinations, and test for threshold and sign-reversal effects.

2. Study area and data

2.1. Overview of the study area

Xiamen City, located in southeastern China (Fig. 2), features a hilly landscape with a mix of mountains, lakes, and coastal zones. The city has a subtropical maritime monsoon climate, with an annual average temperature of 20.9 °C and precipitation of 1388 mm. Its high urbanization rate (90.81%) (Xiamen Municipal Bureau of Statistics & National Bureau of Statistics Xiamen Survey Team, 2024) and advanced digital infrastructure contribute to abundant and spatially rich social media data (SMD), enabling fine-grained analysis of public sentiment in urban parks.

2.2. Data collection and variable categorization

2.2.1. VGI collection and park selection

This study collected volunteered geographic information (VGI) from two major online platforms in China, Dianping and Ctrip. Both platforms allow users to share opinions and impressions about specific locations. Given the large volume of reviews, steady annual growth in active users, and widespread recognition across various research fields (Shang et al., 2023), the data collected from Dianping and Ctrip are regarded as reliable. VGI related to urban parks in Xiamen was collected from both platforms for the period from January 1, 2018, to December 31, 2023. Since the names of some parks did not specify the term 'park' on these platforms, a keyword search for 'park' was performed on Dianping and Ctrip, supplemented by governmental information, including *the Standard for Classification of Urban Green Space (CJJ/T85-2017)* (Ministry of Housing and Urban-Rural Development of the People's Republic of China, 2017), *the List of Parks in Xiamen City (the first batch)* (Xiamen Municipal People's Government, 2013), and other official sources to ensure comprehensive identification of relevant parks. Urban parks with more than 50 comments were selected, resulting in 47 parks being identified for this study.

2.2.2. Categorization of explanatory variables

This study categorizes the explanatory variables influencing park sentiment scores into four primary groups: park structural and locational characteristics, built environment, natural environment, and social environment variables (Juarez et al., 2020). While this study centers on the surrounding environment, park structural and locational characteristics and micro-scale internal environmental quality were incorporated as controls to isolate external influences. Specifically, micro-scale internal environmental quality (marked with an asterisk, *) includes variables like sidewalk density and fractional vegetation cover. Table 1 summarizes the specific variables and their corresponding codes.

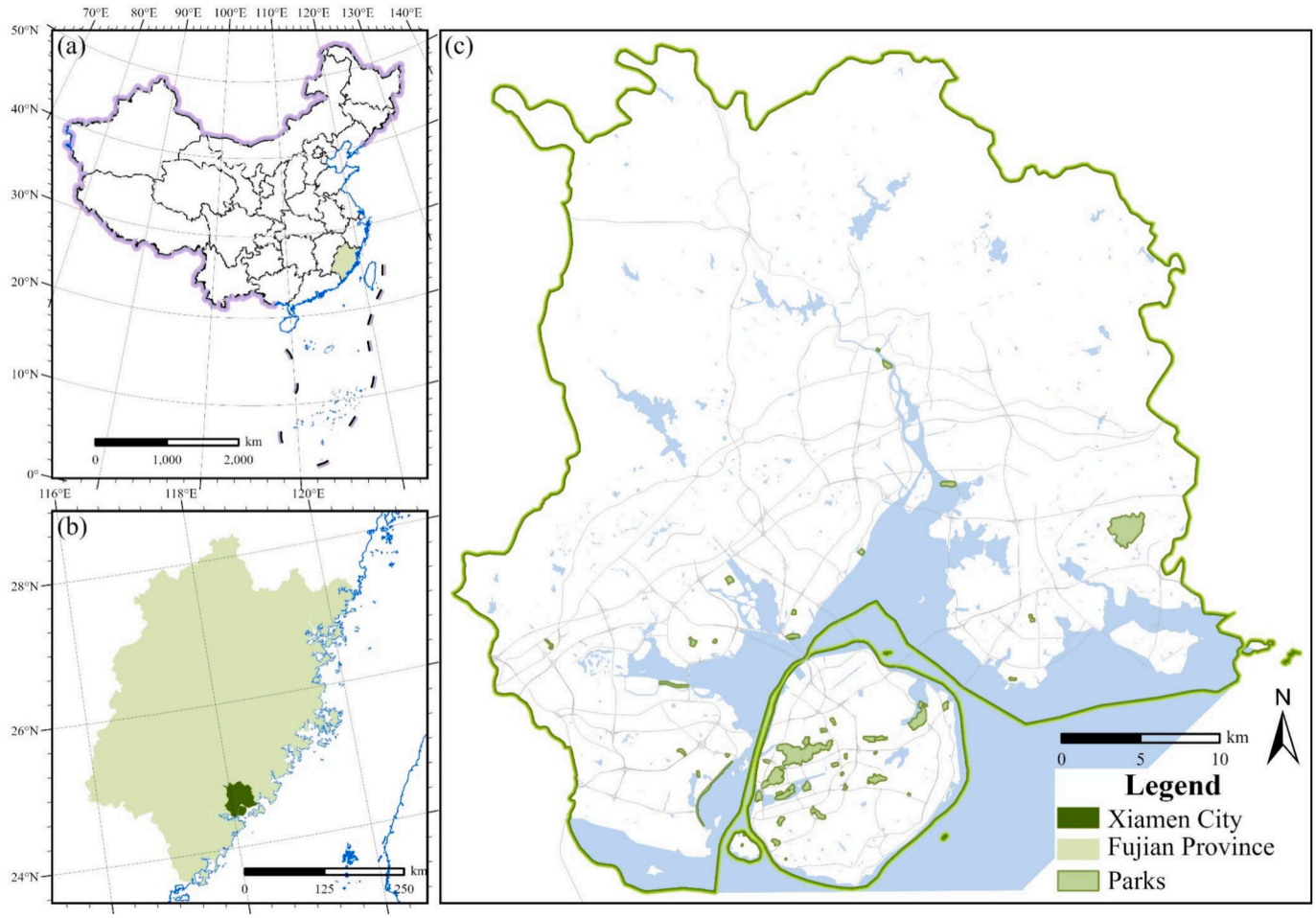

Fig. 2. Geographical location of Xiamen City and the distribution of the studied urban parks.

Table 1
Explanatory variables and corresponding codes.

Variable types	Explanatory variables		Codes
Park structural and locational characteristics	Park size		P_P-SI
	Landscape shape index		P_LSI
	Distance to the city center		P_DTC
Built environment	Road network density		B_RND
	Building height		B_BH
	Sidewalk density*		B_SD
	Driving in 1-h isochronous circles		B_D-1H
	Walking in 7-h isochronous circles		B_W-7H
	Density of facilities and services around parks (SPOI)	Catering services	B_CS
		Public toilets	B_PT
		Shopping facilities	B_SF
		Daily living services	B_DLS
		Recreation services	B_RS
		Parking lots	B_PL
		Accommodation services	B_AS
Natural environment	Fractional vegetation cover*		N_FVC
	Slope*		N_Slope
	Elevation*		N_Elevation
	Distance to water bodies*		N_DWB
Social environment	Population density		S_PD
	Nighttime light intensity		S_NTL

Note: Variables marked with an asterisk (*) denote internal environmental quality at the micro-scale.

3. Methods

3.1. Data preprocessing

All explanatory variables were systematically preprocessed to enhance the reliability of subsequent analyses. N_FVC was obtained from TPDC (Zhao et al., 2023), while N_Slope and N_Elevation were extracted from a Digital Elevation Model (DEM) provided by Tsinghua Cloud (Zhang et al., 2022). S_PD was sourced from Figshare (Chen et al., 2024), and S_NTL was derived from Luojia 1-01 satellite imagery. The variable P_P-SI was calculated based on park-based areas of interest (AOI) data, obtained via the AMap Open Platform, and B_BH was sourced from Zenodo (Wu, 2022). Road variables (B_RND, B_SD) were calculated using OpenStreetMap (OSM) data, aggregated on a 10-m fishnet grid after filtering and topological refinement; SPOI data were also retrieved from AMap and processed using kernel density estimation. Distance variables (P_DTC, N_DWB) were calculated using Euclidean distance to the city center and the nearest major water body. The landscape shape index (P_LSI) was calculated as:

$$LSI = \frac{2\sqrt{\pi^* A}}{P} \tag{1}$$

where LSI is the landscape shape index, A is the park area, and P is its perimeter. Accessibility variables (B_D-1H and B_W—7H) were derived from service area analyses based on OSM road network data, which facilitated the construction of multi-level isochrone service areas.

$$S_f^m(t_1, t_2) = \left\{ x \in \mathbb{R}^2 : t_1 < \min_{p \in P(f,x)} \sum_{e \in p} \frac{L(e)}{V^m(e)} \le t_2 \right\} \tag{2}$$

where $S_f^m(t_1, t_2)$ denotes the set of locations x that are reachable from park f using transportation mode m (either driving or walking) within the time interval $(t_1, t_2]$ (set to 0–1 h for driving and 0–7 h for walking, with multiple interval segments). $P(f, x)$ represents the set of all feasible travel paths from f to x; each path consists of a sequence of edges e, where $L(e)$ is the length of edge e, and $V^m(e)$ is the travel speed on edge e under mode m.

In order to ensure data quality and enhance the accuracy and efficiency of sentiment analysis, this study conducted systematic preprocessing of comment texts. Irrelevant characters, emojis, special symbols, redundant spaces, and line breaks were removed; duplicate, empty, and image-only comments were excluded to ensure data validity. Given the 512-token input limit of the sentiment analysis model, overly long comments were discarded to avoid truncation-related information loss and processing errors. Non-Chinese content in the retained comments was cleaned or translated. After preprocessing, a total of 21,268 valid reviews were obtained for 47 parks, including 2160 from Ctrip and 19,108 from Dianping.

3.2. VGI-based park sentiment assessment

In this study, the "roberta-base-finetuned-dianping-chinese" model (Liu et al., 2019; Zhang & LeCun, 2017; Zhao et al., 2019) was used to compute sentiment scores on VGI related to parks. This model improves upon BERT by training a robustly optimized language model using more data, longer input sequences, dynamic masking, and larger batch sizes over more training steps. Compared to traditional sentiment analysis methods that rely on shallow lexical features or rule-based heuristics, this approach captures deeper contextual semantics and improves generalization, particularly in handling complex or ambiguous texts. The model outputs confidence scores ranging from −1 to 1, indicating sentiment polarity from negative to positive. We applied the following formula to convert them into sentiment scores for the parks.

$$y_{i,t} = \frac{s_{i,t} + 1}{2} \tag{3}$$

where $s_{i,t} \in [-1, 1]$ denotes the raw sentiment confidence score of the t-th comment associated with park i and $y_{i,t} \in [0, 1]$ is the corresponding normalized sentiment score.

$$\overline{y_i} = \frac{1}{M_i} \sum_{t=1}^{M_i} y_{i,t} \tag{4}$$

where $\overline{y_i}$ represents the average sentiment score for park i, reflecting the overall emotional perception derived from VGI, and M_i is the total number of comments related to park i.

3.3. Examining spatial second dimensional association

The SDA method extends traditional first dimension spatial association (FDA) methods (Song, 2022). As shown in Fig. 3, FDA characterizes the geographic environment by aggregating data within a fixed spatial window. Simple aggregation, such as averaging variables within a park's AOI, cannot capture non-monotonic effects across scales and value intervals. For instance, low-quantile nighttime light intensity in the park's near neighborhood and high-quantile nighttime light intensity at the street scale may exert opposite effects on sentiment; similarly, dense road networks immediately adjacent to the park versus high road network density at broader scales may have opposite effects on sentiment. SDA advances this approach by extracting geographic features spanning multiple searching ranges (b) and probability parameters (τ) beyond the sample area, allowing the model to capture such sign-reversing and nonlinear effects across spatial scales and value intervals (see Fig. 3).

In this study's ESDA-based park sentiment driver analysis model, SDA-RF serves as the predictive core. The method consists of four phases, and the first phase aims to characterize the geographic environment using raw-resolution explanatory variable data. SDA-RF supports the integration of multi-resolution data without uniform resampling, enabling direct modeling with raster data at native resolution, thereby preserving the completeness of geographic information.

The second stage combines searching ranges b and probability parameters τ to construct second dimension variables. First, explanatory variables X_i are chosen within varying searching ranges b (e.g., 0.1, 0.5, 2 km) surrounding the park's AOI. Then, probability parameters τ (e.g.,

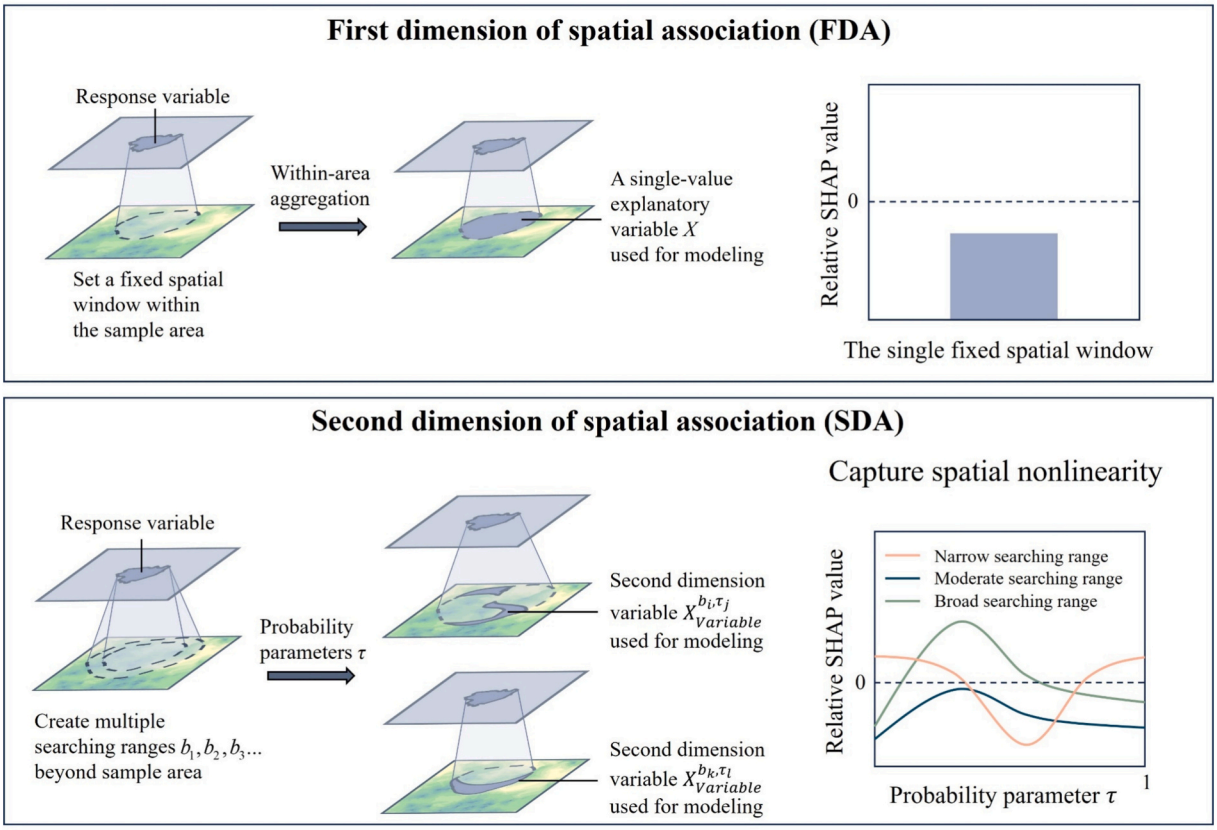

Fig. 3. Comparison of concepts of the first and the second dimensions of spatial association (FDA and SDA).

0, 0.5, 1) are utilized to compute statistical features such as minimum, median, and maximum values, thus generating a series of second dimension variables $X_i(b, \tau)$, to enrich the description of the geographic environment. The searching range b determines the spatial extent of variable influence, while the probability parameter τ is used to extract specific quantile statistics within different ranges of the same base variable. Together, they construct second dimension variables that enable a spatially multi-scaled and non-monotonic response of environmental factors to sentiment scores, thereby embodying the essential nature of a spatially nonlinear function.

The third stage focuses on the selection of second dimension variables. To ensure data quality and model stability, variables exhibiting zero or near-zero variance are first removed, as such variables lack discriminatory power (Kuhn, 2008) and may negatively impact model performance (C & RamaSree, 2015). Following this initial screening, correlation analysis is performed on $X_i(b, \tau)$ to identify variables significantly associated with the response variable, and variables with $p < 0.05$ and $|r| \geq 0.30$ are ranked by the absolute value of their correlation coefficients to form a candidate subset $X'(b, \tau)$. Subsequently, the variance inflation factor (VIF) method is applied to this subset in two stages, first within the candidate variables for each explanatory factor and then across all retained variables globally, to ensure that no severe collinearity exists in the final selected variables $X'(b_p, \tau_q)$. Specifically, variables are introduced into a linear regression model in descending order of their absolute correlation with the response variable. At each step, VIFs are calculated: if all values are below the threshold of 5, the current set is retained; otherwise, the variable with the highest VIF is removed. This iterative process continues until all remaining variables have VIFs below the threshold. The VIF is calculated using the following formula:

$$VIF_i = \frac{1}{1 - R_i^2} \tag{5}$$

where R_i^2 denotes the coefficient of determination obtained when the i-th variable is treated as the response variable, while all other variables serve as explanatory variables in the regression model.

The fourth stage involves modeling and prediction, where we use the random forest model to construct SDA-RF and capture the relationships between environmental variables and park sentiment scores. Random forest is particularly suitable for modeling complex nonlinear interactions and evaluating variable importance, typically by estimating the reduction in prediction error when each variable is included in the model. SDA-RF is specifically expressed as Eq. (6):

$$Y(u) = f\left(X'\left(v, b_p, \tau_q\right)\right) \tag{6}$$

where $Y(u)$ denotes the observation at sample location u, and $X'\left(v, b_p, \tau_q\right)$ is the set of selected second dimension variables at locations v beyond the sample point u, determined by the searching range b_p and the probability parameter τ_q. The function f denotes the learned mapping from predictors to the response as defined by the random forest model.

3.4. Evaluating explainability for the spatial second dimensional association

Owing to the intrinsically opaque nature of random forest algorithms (Teng et al., 2024), it is crucial to employ a transparent and theoretically grounded interpretation framework to understand how individual input features influence model predictions (Zhang et al., 2023). To address the interpretability challenges inherent in the SDA-RF model, we adopted SHAP. SHAP decomposes each model prediction into the sum of additive feature contributions (Shapley values), providing a fair and systematic attribution of the model output (Lapuschkin et al., 2019; Lundberg & Lee, 2017). Mathematically, the SHAP framework represents a prediction $g(x')$ as follows:

$$g(x') = \varphi_0 + \sum_{j=1}^{M} \varphi_j \tag{7}$$

where $g(x')$ is the predicted value of the model, φ_0 is a constant representing the baseline prediction of the model, which is usually the predicted mean value of all training samples, and φ_j is the Shapley value of feature j, i.e., the contribution of the feature to the model prediction.

$$\varphi_j = \sum_{S \subseteq M \setminus \{j\}} \frac{|S|!(M - |S| - 1)!}{M!} [g(S \cup \{j\}) - g(S)] \tag{8}$$

where $|S|$ signifies the number of features in a subset S, M is the total number of features, $g(S)$ is the model prediction with the current set of features, and $g(S \cup \{j\})$ is the predicted value of the model after adding feature j to the subset of features S.

3.5. Model validation

To assess the effectiveness of the SDA-RF model, a comparison with the FDA-RF model was conducted. FDA-RF in this study refers to a method that, without considering geographic information beyond the sample area, aggregates the mean feature values within extracted spatial windows to construct variables and inputs them into the random forest model as explanatory variables. Given the limited size of our dataset, we adopted Leave-One-Out Cross-Validation (LOOCV) for model validation (Stone, 1974). Unlike conventional k-fold or 10-fold validation, LOOCV utilizes each of the n samples exactly once for testing while training on the remaining $n - 1$ samples (Stone, 1974). This strategy provides a more robust and stable assessment for small-sample scenarios (Cheng et al., 2017; Shao & Er, 2016). As screening was not repeated within each LOOCV training fold, the LOOCV metrics may be slightly optimistic; however, our aim is to compare FDA and SDA under an identical predictor set rather than to treat predictive accuracy as the sole objective, so we screened candidate predictors once on the full dataset before running LOOCV to keep the predictor set used for performance evaluation consistent across methods. In terms of model evaluation, R^2 (Eq. (9)), *RMSE* (Eq. (10)), and *MAE* (Eq. (11)) are selected as metrics in this study. Specifically, R^2 reflects the overall goodness of fit, *RMSE* emphasizes large prediction errors, and *MAE* represents the average magnitude of all errors.

$$R^2 = 1 - \frac{\sum_{i=1}^{n} (y_i - \hat{y}_i)^2}{\sum_{i=1}^{n} (y_i - \bar{y})^2} \tag{9}$$

$$RMSE = \sqrt{\frac{1}{n} \sum_{i=1}^{n} (y_i - \hat{y}_i)^2} \tag{10}$$

$$MAE = \frac{1}{n} \sum_{i=1}^{n} |y_i - \hat{y}_i| \tag{11}$$

where y_i denotes the actual sentiment score, $\hat{y}_i$ is the sentiment score predicted by the model, $\bar{y}$ is the average of the actual sentiment scores, and n is the number of samples.

We complemented standard metrics with cross-validated diagnostics to rigorously evaluate generalization. Given the susceptibility to overfitting in this small-sample context characterized by multiple covariates, we scrutinized the empirical distribution of LOOCV residuals (Hastie et al., 2009) and computed Moran's I statistics (Anselin, 1988). These diagnostics were employed to detect systematic bias, heteroscedasticity, and residual spatial autocorrelation. Furthermore, uncertainty in model fit was quantified by deriving 95% confidence intervals for R^2 and *RMSE* based on the distribution of LOOCV predictions (Efron, 1982).

4. Results

4.1. Sentiment scores of urban parks

An analysis of 21,268 comments revealed noticeable differences in public engagement and visitor sentiment among urban parks; nevertheless, the overall feedback remained predominantly positive. The number of comments per park ranged from 50 to 1952, reflecting differing levels of public engagement across parks (see Table A.1). Notably, Bay Park (1919 comments) and Zhongshan Park (1952 comments) received more comments than Guluo Park (51 comments) and Nandi Park (50 comments), suggesting considerable disparities in park visibility or usage. In terms of sentiment, the overall tone was predominantly positive, as reflected by an average sentiment score of 0.788, with 88.19% of comments scoring above 0.5. However, sentiment scores varied notably among parks. Specifically, fourteen parks recorded mean sentiment scores above 0.8, twenty parks fell between 0.7 and 0.8, and twelve between 0.6 and 0.7, with only one park falling below 0.6. Among them, Susong Memorial Park (0.865) and Yundang Lakeside Linear Park (0.863) received the most favorable evaluations. In contrast, Yanwu Park (0.532) and Jinshang Park (0.615) were among the lowest-rated, indicating substantial variation in perceived visitor satisfaction.

While the number of parks varies across administrative districts, the overall level of visitor experience remains relatively balanced (Fig. 4). Siming District contains the most parks (18), followed by Huli (10), Haicang and Jimei (each with 6), Xiang'an (4), and Tong'an (3), reflecting an uneven spatial distribution. Nevertheless, sentiment scores across districts ranged narrowly from 0.725 to 0.812, suggesting a consistently high quality of visitor experience citywide. Tong'an District recorded the highest average score (0.812), while Jimei had the lowest (0.725), a modest difference of only 0.087.

4.2. Variable selection and modeling

To elucidate the spatially nonlinear effects of environmental variables on park sentiment, a comprehensive process involving variable generation, screening, and final model construction was implemented based on SDA-RF. The variable generation method of SDA-RF retains the native spatial resolution and avoids resampling, in contrast to FDA-RF, which requires data resampling prior to variable generation. Variables were reclassified based on experimental design considerations (see Appendix B), and tailored generation strategies were adopted for different categories (see Appendix C). To simplify notation, SDA variables capturing the surrounding environment are denoted as $X^{b,\tau}_{Variable}$, and untransformed non-SDA variables describing within-park conditions are denoted as $P_{Variable}$ or $P^{\tau}_{Variable}$ throughout the remainder of this paper, where *Variable* represents the base variable code (e.g., S_PD, B_BH), b denotes the searching range, and τ is the probability parameter. A total of 2918 variables were generated, comprising 2860 second dimension variables $X^{b,\tau}_{Variable}$ and 58 untransformed non-SDA variables $P_{Variable}$ and $P^{\tau}_{Variable}$, which were then used for variable selection. In the variable screening stage, 301 (10.3%) low-information SDA variables were excluded based on zero variance and near-zero variance criteria. The removal process revealed strong sensitivity of several second dimension variables to searching ranges (b), probability parameters (τ), and variable-specific attributes, as detailed in Appendix D. After correlation analysis and VIF-based screening, a total of 20 SDA variables and 4 non-SDA variables were ultimately selected for training the random forest model. Fig. 5 shows the 20 screened surrounding environmental variables $X^{b,\tau}_{Variable}$, including B_BH, B_CS, B_D—1H, B_RND, B_W—7H, S_NTL, S_PD, along with their optimal searching ranges b and probability parameters τ, and their relative importance values in the random forest model.

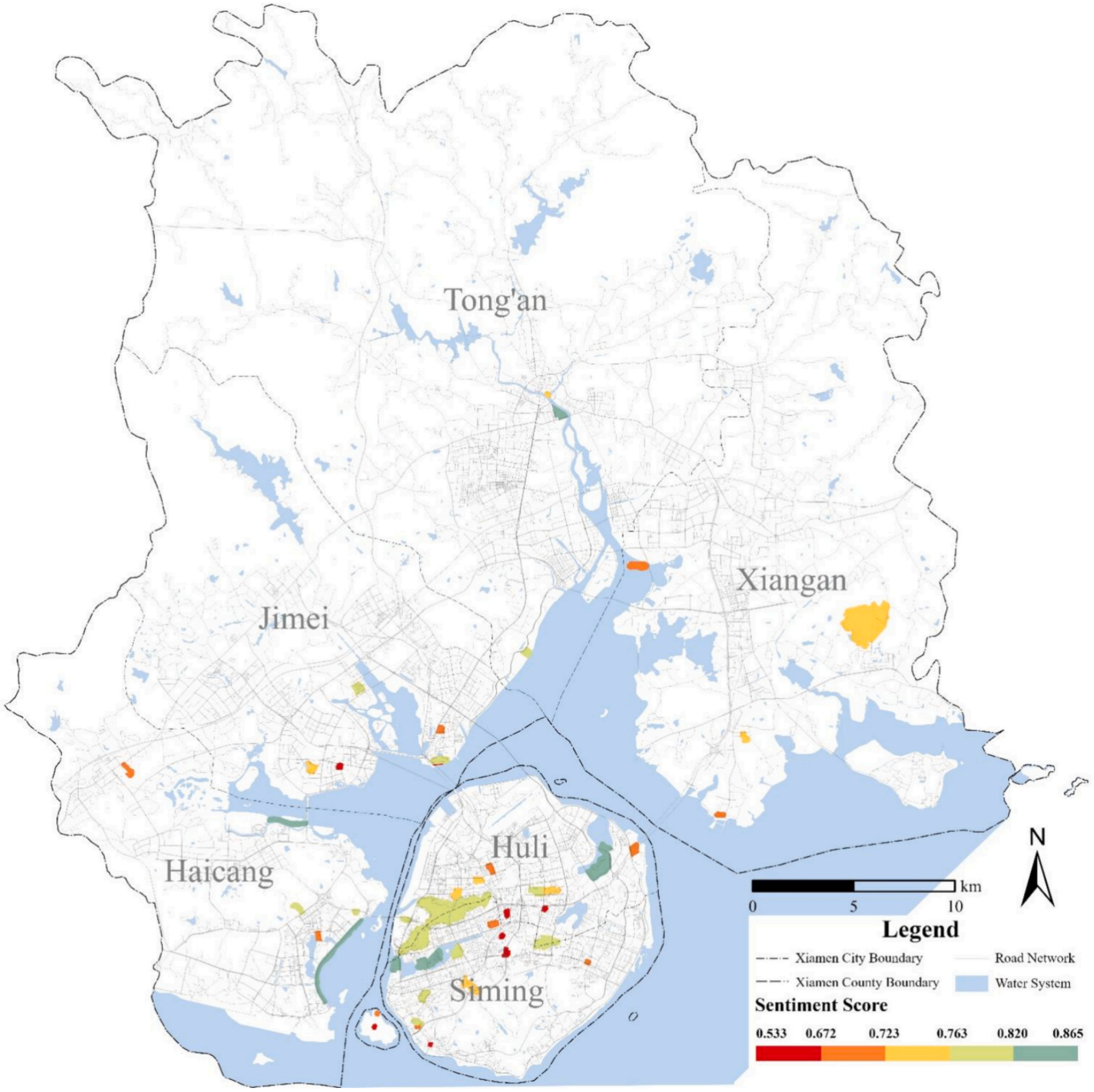

Fig. 4. Spatial distribution of park sentiment derived from VGI using the RoBERTa model.

4.3. Relationship between park sentiment score and influencing factors

Drawing on the SDA-RF model, we applied SHAP analysis to quantify the marginal contributions of each explanatory variable to sentiment predictions and, by means of matrix heatmaps (Fig. 6a) with search radius (b) on the vertical axis and probability parameter (τ) on the horizontal axis, visualized the normalized relative SHAP values of all second dimension variables derived from four representative surrounding environmental factors (B_RND, B_BH, S_NTL, S_PD), thereby characterizing their spatially nonlinear effects in the scale–distribution space. Fig. 6b further presents the top 15 key features ranked by mean absolute Shapley value together with their individual contribution patterns, in order to elucidate the underlying influence mechanisms of the second dimension variables. $P_{P\_P\_SI}$, $P^{\tau=0}_{N\_FVC}$, P_{P_DTC}, and P_{P_LSI} ranked 1st, 10th, 11th, and 13th in variable importance, respectively, indicating that scale and location, along with internal park environmental characteristics, were effectively captured by the model. After controlling for these differences, the contribution of surrounding environmental factors as external drivers of inter-park sentiment differences becomes clearer.

Fig. 6a(i) shows a spatially nonlinear pattern of road network density, with sign reversals spanning spatial scales, characterized by strong inhibition at the immediate interface, weakened effects at mid-range distances, and pronounced positive gains at larger spatial scales. The SHAP ranking in Fig. 6b further demonstrates that high road network density at the larger scale ($X^{b=2.0,\tau=1.0}_{B\_RND}$ ranks third) manifests a strong positive gain, with high feature values widely dispersed along the positive axis. Such positive correlation aligns with the view that developed transport networks foster positive outcomes via accessibility

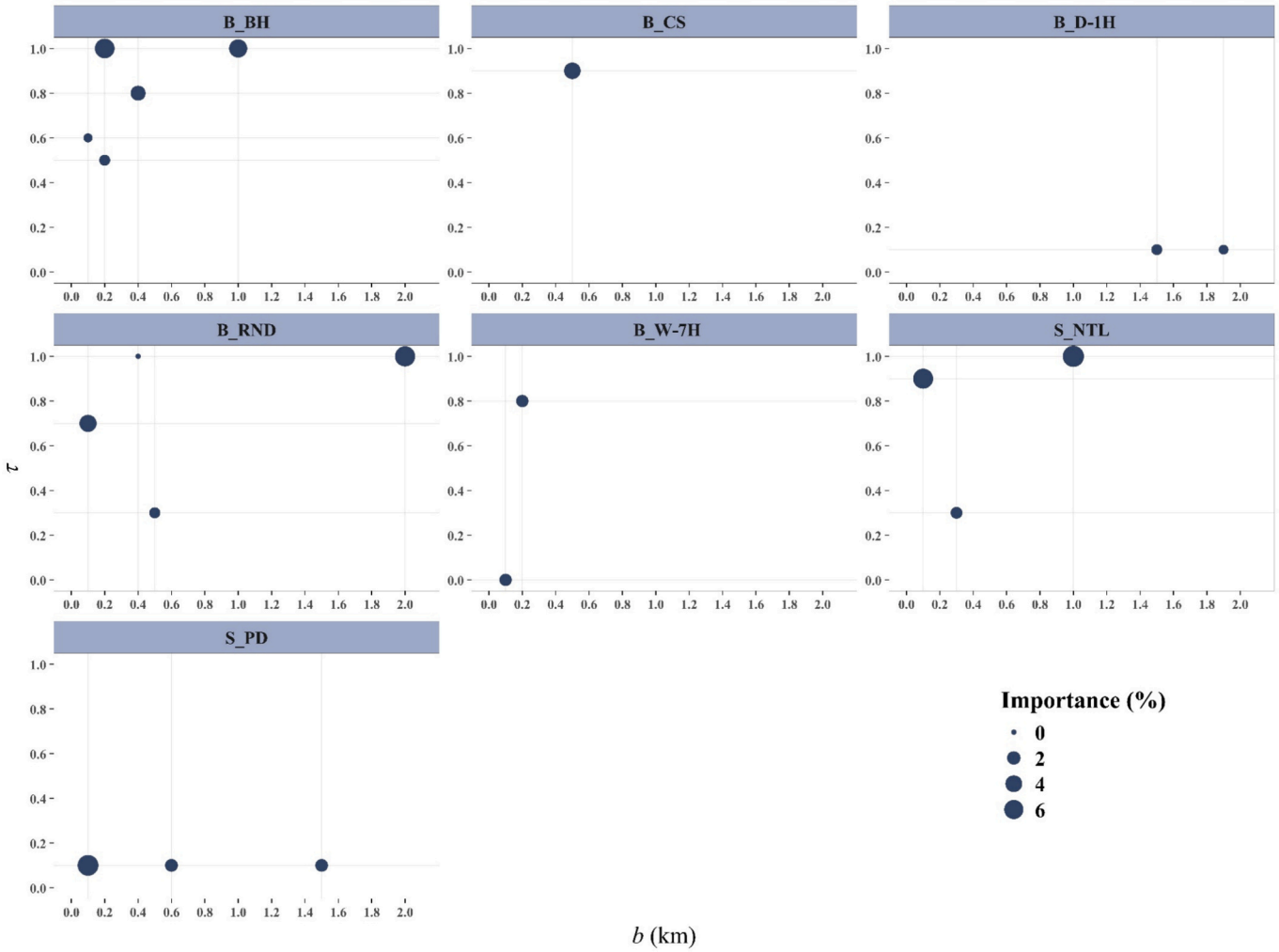

Fig. 5. Relative importance values of selected second dimension variables in the random forest model, with corresponding optimal searching ranges (b) and probability parameters (τ).

mechanisms at larger spatial scales, which previous studies identify as critical for visitor satisfaction (Fan et al., 2021; Li et al., 2025). At the immediate neighborhood scale, medium-to-high quantiles of road network density ($X_{B\_RND}^{b=0.1,\tau=0.7}$ ranks eighth) exhibit a distinct negative correlation, with the inhibitory effect of high values substantially more pronounced than the limited positive contribution driven by low values, demonstrating a clear sign reversal relative to the larger-scale effect. Dense road networks adjacent to parks likely function primarily as environmental burdens (e.g., noise and safety hazards). Long-term traffic noise exposure poses health risks to people inside green spaces and affects restorative experiences (Payne, 2008; Zhu & Chen, 2023). At the mid-range scale, high-density road networks ($X_{B\_RND}^{b=0.4,\tau=1.0}$ ranks 15th) yield modest positive gains, suggesting that connectivity benefits of network density begin to offset environmental disturbance within this spatial scale. By contrast, low-quantile road network density at the same scale $X_{B\_RND}^{b=0.5,\tau=0.3}$ shows much weaker effects, indicating that the influence of road network density is driven primarily by high-quantile conditions.

Fig. 6a(ii) shows that the sentiment effect of high-rise buildings is highly scale-sensitive and non-monotonic: it is weakly negative at 0.2 km while high values still contribute positively, becomes most negative at 0.4 km, and then weakens at 1 km with positive contributions persisting for high values. High-rise buildings at the near-neighborhood scale ($X_{B\_BH}^{b=0.2,\tau=1.0}$ ranks 7th) overall exhibit a weak negative effect, but a large share of high values is still clustered along the SHAP positive axis. Within Xiamen's hot-humid climate, shading from adjacent high-rise buildings may substantially improve thermal comfort, and prior studies have shown that such thermal benefits tend to dominate micro-scale user experiences (Lin et al., 2010). When the spatial buffer expands ($X_{B\_BH}^{b=0.4,\tau=0.8}$ ranks 14th), the negative effect intensifies, potentially stemming from visual obstruction or noise disturbance associated with high-rise development. These observations align with previous studies showing that excessively tall buildings can intensify feelings of enclosure and oppression (Chung et al., 2022; Lindal & Hartig, 2013; Zarghami et al., 2019). At the 1 km scale, maximum building height ($X_{B\_BH}^{b=1.0,\tau=1.0}$ ranks 6th) shows a comparatively weak negative effect, as its influence is diluted by scale expansion, thereby reducing its adverse impact on visitor experience. Although the mean SHAP value is negative, most of the high values of this feature are still distributed along the positive axis, likely stemming from the denser service provision associated with high-rise buildings, which enhances perceived security and convenience (Lee, 2011; Li et al., 2023). This pattern aligns with prior evidence: in compact urban environments, the need for psychological detachment strengthens the restorative potential of green spaces, making them more valuable within high-rise settings (Nordh et al., 2009). By contrast, mid-rise buildings at the near-neighborhood scale ($X_{B\_BH}^{b=0.2,\tau=0.5}$ and $X_{B\_BH}^{b=0.1,\tau=0.6}$) have only weak effects on visitor experience.

Fig. 6a(iii) shows that S_NTL exhibits a quantile-asymmetric effect of

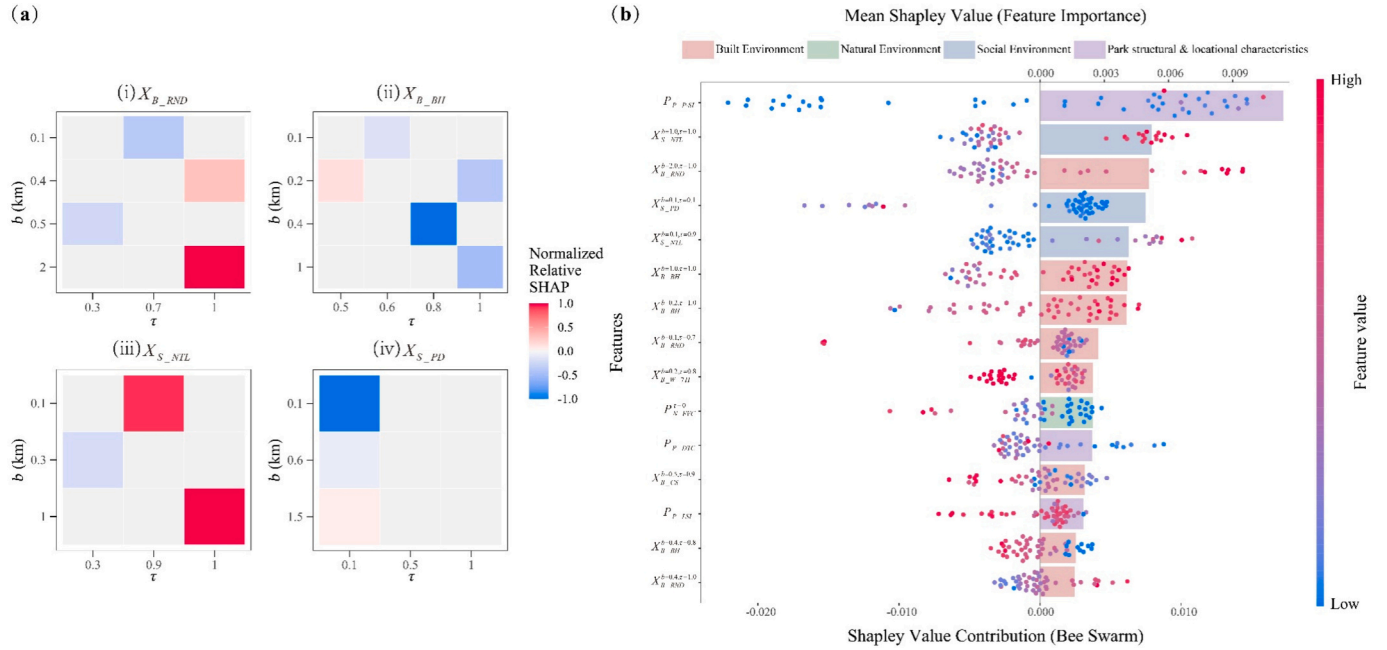

Fig. 6. Interpretability analysis of SDA-RF integrating scale–quantile heatmaps, a SHAP beeswarm summary plot, and feature-importance bars to illustrate spatially nonlinear effects of environmental factors on park sentiment. (a) Matrix heatmaps of mean relative SHAP values for four representative second dimension predictors, B_RND (i), B_BH (ii), S_NTL (iii), and S_PD (iv), with the probability parameter τ on the x-axis and the searching range b (km) on the y-axis. Values are normalized within each predictor to [−1,1] for pattern comparison; positive/negative values indicate that the predictor increases/decreases the model's predicted sentiment relative to the baseline prediction. (b) SHAP beeswarm plot with mean absolute SHAP bars summarizing feature importance and sample-level contributions: the lower x-axis shows SHAP values, the upper x-axis shows mean |SHAP|.

nighttime light: high peaks in illumination enhance sentiment evaluations, whereas an overall elevation of low-quantile levels turns its beneficial influence into a source of disturbance. The positive effect of high nighttime light at both 1 km and 0.1 km scales is strong ($X_{S\_NTL}^{b=1.0,\tau=1.0}$ ranks second; $X_{S\_NTL}^{b=0.1,\tau=0.9}$ ranks fifth), where high values exhibit a broad dispersion along the positive axis. This result suggests that parks embedded in highly vibrant areas with dense service provision at the 1 km scale, and with well-illuminated entrances and surrounding roads at neighborhood walking scale, are more likely to receive positive evaluations. Consistent with this result, previous studies have pointed out that artificial lighting can promote nighttime leisure activities, social interaction and perceived safety (Gaston et al., 2015). Meanwhile, the positive effect of nighttime light greatly weakens and even becomes slightly negative as τ decreases to 0.3 ($X_{S\_NTL}^{b=0.3,\tau=0.3}$), suggesting that when lower-quantile nighttime light around park boundaries is relatively high, excessive nighttime activity in adjacent areas can act as a disturbance, suppressing sentiment scores.

Fig. 6a(iv) shows that the influence of surrounding population density on park sentiment is highly scale-dependent, producing strong suppressive effects in the near neighborhood while rapidly attenuating and shifting toward neutral or mildly positive impacts at larger scales. The near-neighborhood baseline of population density ($X_{S\_PD}^{b=0.1,\tau=0.1}$ ranks fourth) exhibits a long-tailed distribution, with a large cluster of low values concentrated along the SHAP positive axis, while high values extend broadly along the negative axis. The pattern suggests a pronounced suppressive effect of excessive population density. A higher minimum population density implies persistently intense activity in the near neighborhood, likely increasing crowding and noise exposure and thereby lowering visitors' sentiment evaluations. Experimental research indicates that high-density crowds often encroach upon personal space, inducing negative emotions such as stress and anger (Engelniederhammer et al., 2019). Consistent with this mechanism, studies on Shanghai urban parks have further revealed a negative correlation between surrounding population density and park-use experiences derived from social media data (Huai et al., 2023). At larger spatial scales ($X_{S\_PD}^{b=0.6,\tau=0.1}$ and $X_{S\_PD}^{b=1.5,\tau=0.1}$), the negative effect rapidly attenuates toward neutrality or a weakly positive direction, supporting the highly localized nature of population-density interference with visitor experience. These results suggest that, beyond a certain scale threshold, increases in the lower end of area-wide population density may promote baseline urban vitality and potential support for social interaction. This interpretation is supported by previous studies. A broader population context can better align with visitors' social needs (Chiesura, 2004) and help avoid insecurity associated with overly deserted environments (Jacobs, 1992), thereby improving park visitors' mood.

The same factor shifts in direction and magnitude across different combinations of scales and value ranges, giving rise to sign reversals and threshold effects. Sentiment responses are therefore no longer a linear function of scales or average levels, but an integrated response to the structure of multi-scale and multi-level environmental exposures. External built and social environments are coupled through mechanisms such as accessibility, visual obstruction, urban vitality and perceived safety operating at different scales and value ranges, and jointly shape inter-park sentiment differences.

4.4. Result of model validation

This study examined the methodological distinctions between FDA-RF and SDA-RF in the process of variable construction to validate the effectiveness of SDA-RF. Fig. 7 compares the variable importance rankings for predicting sentiment scores generated by the two models. The comparison reveals that, unlike FDA-RF, SDA-RF mines more detailed and multidimensional variable contributions in the importance ranking results. For instance, the variable importance ranking in the FDA-RF model exhibits a high degree of concentration, with the P_P-SI variable playing a dominant role, while factors such as S_PD show relatively lower importance, and B_BH is absent from the top feature list. In contrast, the SDA-RF model demonstrates a more balanced

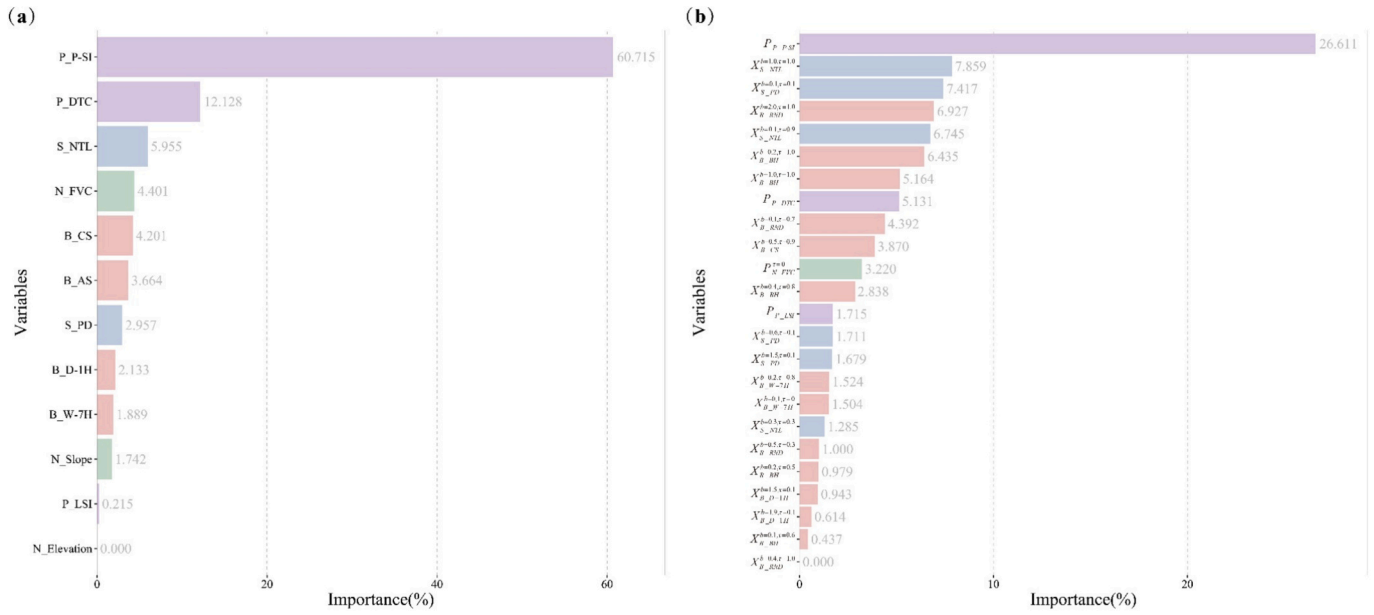

Fig. 7. Comparison of explanatory variable importance rankings between FDA-RF and SDA-RF for predicting sentiment scores. Bar colors represent feature types: pink (built), green (natural), blue (social), and purple (park structural and locational characteristics). (For interpretation of the references to color in this figure legend, the reader is referred to the web version of this article.)

distribution of variable importance. Multiple second dimension variables originating from S_PD and B_BH exert influence across different hierarchical levels. This suggests that SDA-RF, through the construction of second dimension variables, is not only capable of revealing spatially nonlinear mechanisms, but also of uncovering more complex structures of environmental influence and mitigating the overdominance of individual factors in model outcomes.

To evaluate model performance, the predicted values generated by FDA-RF and SDA-RF were compared against observed values using multiple statistical metrics. Fig. 8 illustrates the comparison between the predicted and observed values of FDA-RF and SDA-RF. Overall, the SDA-RF model exhibits a better fit to the observed data compared to the FDA-RF model, as evidenced by a more centralized distribution of predicted points and reduced prediction errors. The cross-validation results indicate that SDA-RF outperformed FDA-RF on several key performance indicators, demonstrating better prediction capability (Table 2). Specifically, the coefficient of determination (R^2) for the SDA-RF model is 0.459, representing a 28.57% improvement over the FDA-RF model's R^2 of 0.357, thereby indicating a more accurate representation of the variance in the observed data. In addition, the root mean square error (*RMSE*) and mean absolute error (*MAE*) of SDA-RF are reduced by 8.93% and 6.82%, respectively. Lower RMSE values reflect reduced error fluctuation during prediction, while the decrease in *MAE* further proves that the model has improved the overall prediction accuracy.

Table 2
Improvements of model accuracy by SDA-RF compared with FDA-RF.

Model	R^2	95% CI of R^2	RMSE	95% CI of RMSE	MAE
FDA-RF	0.357	0.14–0.50	0.056	0.044–0.069	0.044
SDA-RF	0.459	0.29–0.57	0.051	0.041–0.062	0.041
Improvement by SDA (%)	28.57		−8.93		−6.82

Given the small sample of 47 parks and the large set of engineered predictors, we evaluated generalization with LOOCV diagnostics.

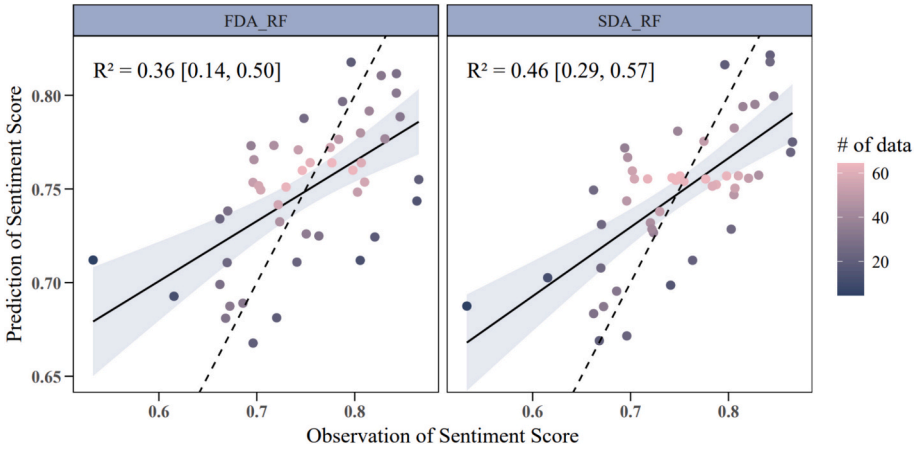

Fig. 8. Observed versus LOOCV-predicted park sentiment scores for FDA-RF and SDA-RF. Each point represents an out-of-sample prediction for one park obtained from leave-one-out cross-validation. The dashed line denotes the 1:1 reference (perfect agreement), and the solid line shows the fitted regression with the 95% confidence band (shaded). R^2 with its 95% CI is reported in each panel (FDA-RF: left; SDA-RF: right).

LOOCV residuals (observed minus predicted) are centered near zero and mostly fall within ±0.10 for both models (Fig. 9a–b). No pronounced fan-shaped dispersion is observed in the residual plots, suggesting limited heteroscedasticity (Fig. 9c–d). Residuals show a mild calibration shrinkage pattern, with overestimation at the lower end and underestimation at the higher end of observed scores, which is expected for bounded outcomes under ensemble regression and LOOCV rather than indicative of high-variance overfitting. Residual spatial autocorrelation is weak, with Moran's I close to zero and not significant for either model (FDA-RF: $I = -0.105$, $p_{perm} = 0.837$; SDA-RF: $I = -0.0585$, $p_{perm} = 0.639$). As shown in Table 2, LOOCV-based 95% confidence intervals for R^2 and RMSE are within a reasonable range, indicating non-trivial and reasonably stable predictive performance.

5. Discussion

5.1. Diagnosing spatial nonlinearity in human–environment interactions

Park sentiment does not respond to surrounding environments in a simple linear manner; instead, it exhibits complex and structured spatial nonlinearity in response to environmental exposures. In this VGI-based analysis of urban park sentiment, we adopt an ESDA model to diagnose the spatially nonlinear pattern through which surrounding environmental factors influence visitor sentiment across different combinations of spatial scales and value intervals. Methodologically, ESDA constructs second dimension variables by combining the searching range b with the probability parameter τ, where lower quantiles represent baseline conditions and higher quantiles capture extreme high exposures; SHAP is then used to interpret both the overall and fine-grained response patterns of these second dimension variables. Our main contribution is the empirical finding that, after controlling for within-park conditions, surrounding built and social exposures relate to park sentiment nonlinearly across spatial scales and value intervals. Using the ESDA model, we address a key limitation of prior human–environment studies that rely on fixed neighborhoods and single-summary aggregation and thus struggle to identify scale nonlinearity and value-distribution nonlinearity simultaneously.

5.2. Spatially nonlinear effects of surrounding built and social factors on park sentiment

Our analysis uncovers that environmental influences are highly contingent on specific combinations of scale and value distribution, primarily manifesting as sign reversals and thresholds in four key factors. In terms of the physical built environment, road network density and building height primarily manifest as sign reversals. Road network density exhibits a sign reversal from near-neighborhood negative suppression to broader-scale positive gains: the positive association between large-scale road network accessibility and satisfaction is consistent with existing studies and theoretical expectations (Fan et al., 2021; Li et al., 2025), whereas dense road networks in the immediate vicinity undermine the benefits of accessibility through noise and other environmental burdens (Payne, 2008; Zhu & Chen, 2023), moving beyond earlier assumptions that treated road network density as a purely positive factor. Accordingly, effective planning requires a tiered approach: facilitating area-wide access through medium-to-high regional network density, while moderating density at the immediate interface to attenuate noise and safety risks. Building height is likewise

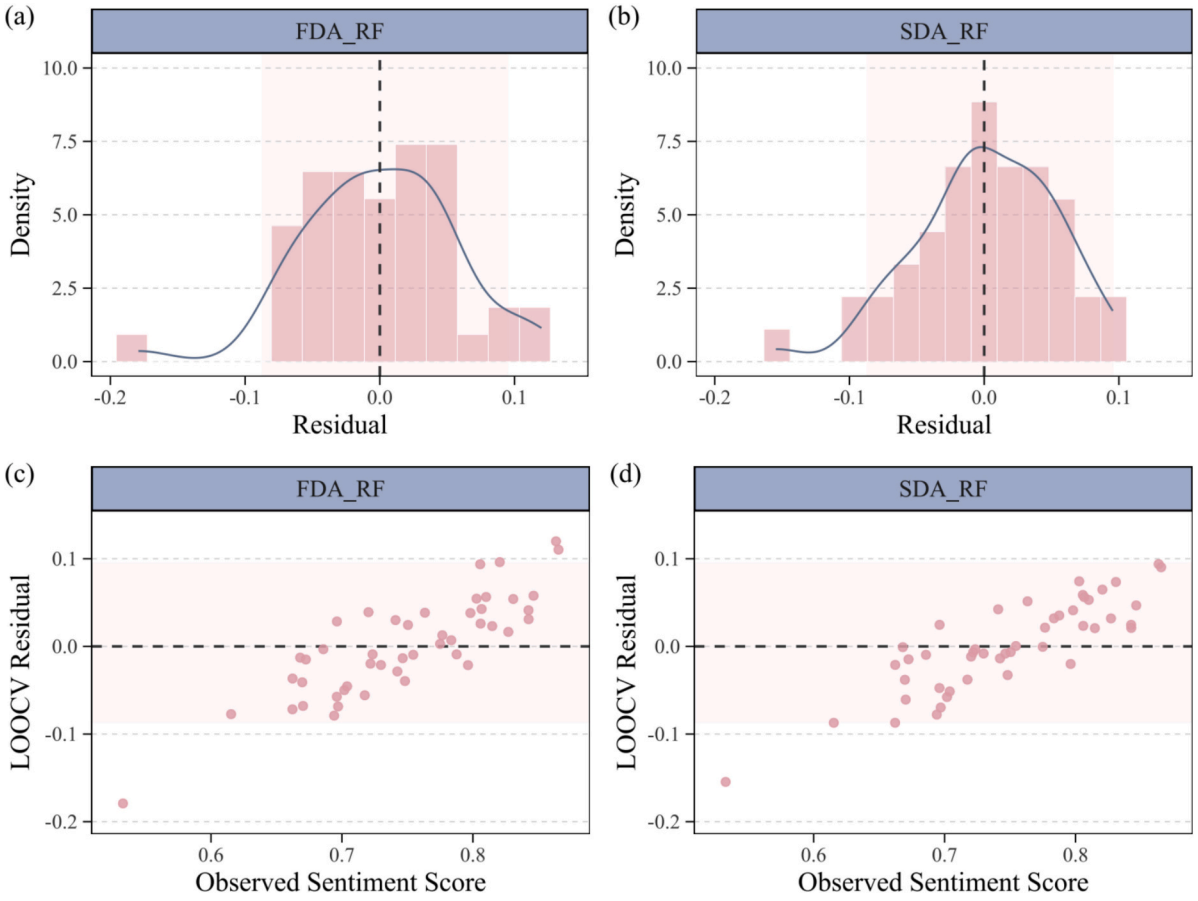

Fig. 9. LOOCV residual diagnostics for assessing systematic bias and overfitting risk in FDA-RF vs. SDA-RF. (a–b) Distributions of LOOCV residuals for FDA-RF and SDA-RF; the dashed vertical line marks zero residual. (c–d) LOOCV residuals plotted against observed sentiment scores; the dashed horizontal line marks zero residual.

highly scale-dependent: at micro scales, mid- to high-rise buildings may improve thermal comfort through shading, but they may also induce visual oppression and noise disturbance, corresponding respectively to experimental evidence and environmental psychology discussions of their positive and negative perceptions (Chung et al., 2022; Lin et al., 2010; Lindal & Hartig, 2013; Zarghami et al., 2019); at larger scales, greater building height signals the clustering of services and functions and is associated with perceived improvements in safety and convenience (Lee, 2011; Li et al., 2023), expanding the discourse on building height from embodied perception to convenience and safety. Thus, parks appear well-suited to districts where sub-district scale high-rise landmarks align with service agglomeration to support perceived safety and convenience, while simultaneously balancing spatial enclosure and shading regulation effects at the immediate scale.

Regarding social and activity intensity, nighttime light intensity and population density exhibit pronounced quantile sensitivity and scale dependence, respectively. Both in the near-neighborhood of parks and at larger scales, higher-quantile illuminance is generally accompanied by more positive sentiment evaluations, consistent with findings that appropriate artificial lighting enhances nighttime vitality and perceived safety (Gaston et al., 2015); when lower-quantile illuminance is uniformly elevated to high levels, however, intense nighttime activity near park boundaries generates noise and visual disturbance, suggesting a context-dependent interference threshold for lighting. This suggests that high overall illuminance at the sub-district scale can serve as a useful macro-level baseline, while higher-quantile illuminance within the micro-perception zone helps enhance visibility. By contrast, avoiding excessive baseline illuminance at the neighborhood-walkable scale helps cultivate a more transitional light environment. Population density displays a scale-dependent pattern: at near-neighborhood scales, increases in baseline population density imply persistently intense pedestrian flows that, through crowding and noise exposure, markedly depress sentiment evaluations (Engelniederhammer et al., 2019); as scale expands, its negative effects weaken rapidly and tend toward neutral or mildly positive, reflecting the indirect role of density in supporting safety and social opportunities (Chiesura, 2004; Jacobs, 1992) rather than indicating that density is uniformly beneficial or detrimental. In response, park siting should favor locations with moderate baseline population density in the immediate neighborhood to allow buffer space against micro-scale crowding, while being situated within a broader hinterland with a sufficient population base to support social vitality. In conclusion, these results align with established theory and prior evidence, but advance the literature by showing that sentiment associations with surrounding built and social exposures depend on specific scale–distribution combinations. Relationships that appear stable under fixed-neighborhood summaries can show sign-reversing threshold-like responses when scale and value distribution are considered jointly.

5.3. Limitations and future research

Future studies are recommended from the following aspects based on the developed ESDA model and the findings from this study. First, future research can improve data representativeness by combining social media-derived sentiment with complementary data sources such as surveys or interviews. Social media expressions tend to emphasize positive self-presentation (Hjetland et al., 2022), and user participation is uneven across age groups, with younger and middle-aged users being more active than older populations (Widener & Li, 2014). Integrating multiple data sources enables a more balanced characterization of public evaluations and allows comparison of sentiment patterns between online and offline populations under different social contexts. Second, future studies can apply the ESDA model to larger and more diverse urban systems. Extending the analysis to multiple cities with different climatic conditions, urban morphologies, and development stages allows systematic examination of whether the identified spatially nonlinear response patterns persist across geographic contexts or vary with environmental and structural settings. Multi-city applications also support evaluation of the stability of spatial mechanisms under different sample sizes and spatial configurations. Third, future research can further validate the ESDA model through broader empirical testing. Applying the model to expanded datasets enables comparative assessment of spatial mechanisms across regions and facilitates examination of uncertainty propagation under different spatial structures. Such large-scale validation contributes to a more comprehensive understanding of the general applicability of the identified spatial relationships. Finally, future studies can extend the ESDA model by integrating it with alternative spatial modeling approaches. Methods such as Geographically Weighted Regression (GWR) (Brunsdon et al., 1996) and Multiscale Geographically Weighted Regression (MGWR) (Fotheringham et al., 2017) can be incorporated to examine spatially varying relationships under second dimension exposure representations. In addition, advances in sentiment analysis models and multimodal data integration provide opportunities to improve analytical precision when handling complex linguistic expressions such as sarcasm and irony.

6. Conclusions

This study conceptualizes park sentiment as a spatially nonlinear response arising from interactions between exposure scales and value ranges of surrounding environments, develops an explainable ESDA model for characterizing such nonlinear responses, and implements the model in addressing park sentiment patterns in Xiamen. The ESDA model represents surrounding environments using b-τ combinations, which jointly encode spatial scale and value distribution, and integrates SHAP to identify directionally interpretable and sign-reversing effects that are not captured by fixed-neighborhood or mean-based representations. The results show that ESDA improves predictive performance and produces more balanced interpretations than conventional FDA-based representations, particularly under small-sample conditions. The findings indicate that surrounding built and social environments influence park sentiment through structured spatial nonlinearity rather than uniform or monotonic effects. Key external factors exhibit scale- and quantile-dependent reversals, suggesting that the same environmental feature can function as either a benefit or a disturbance depending on its spatial context. For readers and practitioners, these results support a tiered understanding of park siting and surrounding-environment management, emphasizing the need to balance near-interface disturbance control with broader-scale accessibility, vitality, and safety. Future studies should examine the transferability of the identified b-τ mechanisms across cities with different urban forms and larger samples, and extend the ESDA model to other spatial learning approaches.

CRediT authorship contribution statement

Xiaojun Wang: Writing – original draft, Visualization, Methodology, Formal analysis, Data curation, Conceptualization. **Yilong Wu:** Writing – original draft, Visualization, Methodology, Formal analysis, Data curation, Conceptualization. **Tingyu Shi:** Writing – review & editing, Formal analysis. **Rongyu Zhang:** Writing – review & editing, Formal analysis. **Yanxi Chen:** Writing – review & editing, Formal analysis. **Yongze Song:** Writing – review & editing, Supervision.

Declaration of competing interest

The authors declare that they have no known competing financial interests or personal relationships that could have appeared to influence the work reported in this paper.

Acknowledgments

The authors would like to thank Dr. Peng Luo from the Senseable City

Laboratory at the Massachusetts Institute of Technology (MIT) for his valuable suggestions on the writing and structure of this paper.

Appendix A. Online review statistics and sentiment scores of urban parks in Xiamen

Table A.1
Statistics of online review volume and RoBERTa-derived sentiment scores for Xiamen urban parks based on Dianping and Ctrip data.

Park	Number of comments	Mean sentiment score	Park	Number of comments	Mean sentiment score
Bailuzhou Park	1699	0.84253	Nandi Park	50	0.670306
Bishan Hill Park	83	0.662303	Nanhu Lake Park	997	0.814746
Buzheng Park	56	0.662219	Qianpujianshen Park	102	0.696169
Caijianwei Mountain Park	448	0.783492	Ridong Park	105	0.746384
Daping Hill Park	961	0.805566	Sanjiangkou Hot Spring Wetland Park	131	0.697053
Guluo Park	51	0.763342	Dongdulijiao Park	223	0.798089
Haicang Bay Park	486	0.827031	Xiamen Children's Park	181	0.70182
Bay Park	1919	0.842433	Shitoupi Mountain Park	53	0.740923
Hongshan Hill Park	552	0.806634	Shuangxi Park	86	0.750441
Huwei Hill Park	780	0.796255	Songbai Park	211	0.696084
Huli Park	301	0.742292	Susong Memorial Park	79	0.865352
Hutou Mountain Park	128	0.754437	Old Railway Park	1210	0.685799
Huaiyuan Park	59	0.721825	Wutong Lighthouse Park	456	0.694063
Torch Park	78	0.7234	Wuyuan Bay Wetland Park	1545	0.846311
Jimeishimin Park	121	0.774938	Xiatianwei Mangrove Wetland Ecological Park	327	0.717428
Jiangtou Park	206	0.672454	Xianyue Park	518	0.805866
Jinbang Park	474	0.748137	Xiangshan Hill Park	626	0.72979
Jinshang Park	51	0.615384	Xingdong Park	95	0.66969
Tan Keng-hean Park	143	0.703933	Xueling Mountain Park	350	0.776665
Lianhua Park	165	0.668109	Yanwu Park	75	0.532828
The Lake of Dragon Boat	699	0.787551	Yanwei Hill Eco-Park	91	0.72025
Belt-shaped Park around Maluan Bay	217	0.830822	Yundang Lakeside Linear Park	288	0.863455
Meifeng Park	102	0.820489	Zhongshan Park	1952	0.80278
Zhonglun Park	983	0.810065			

Appendix B. Reclassification of explanatory variables

Explanatory variables differ in the type of data and the scope of influence on park sentiment, so this study once again categorized the explanatory variables according to the specific needs of the experiment (see Table B.1). The first type of variables refers to park characteristics, including park size (P_P-SI), landscape shape index (P_LSI), and distance to the city center (P_DTC), which are intrinsic attributes of parks and correspond to only one unique characteristic value for each park. The second category of variables is the raster variables within the AOI of parks, which have less influence outside the park and more influence on the sentiment score inside, such as fractional vegetation cover (N_FVC), distance to water bodies (N_DWB) and sidewalk density (B_SD). The third category comprises park peripheral raster variables. Compared with the second category, these variables are summarized within the area between the park boundary and the outer buffer boundary to represent the influence of the surroundings outside the park AOI on sentiment scores, such as road network density (B_RND) and population density (S_PD).

Table B.1
Reclassification of explanatory variables.

	Explanatory variables
First-class variables	Park size (P_P-SI)
	Landscape Shape Index (P_LSI)
	Distance to the city center (P_DTC)
Second-class variables	Sidewalk Density (B_SD)
	Fractional Vegetation Cover (N_FVC)
	Slope (N_Slope)
	Elevation (N_Elevation)
	Distance to Water Bodies (N_DWB)
Third-class variables	Road Network Density (B_RND)
	Building Height (B_BH)
	Driving in an isochronous circle (B_D-1H)
	Walking in an isochronous circle (B_W-7H)
	Catering Services (B_CS)
	Public Toilets (B_PT)
	Shopping Facilities (B_SF)
	Daily Living Services (B_DLS)
	Recreation Services (B_RS)
	Parking Lots (B_PL)

(*continued on next page*)

Table B.1 (*continued*)

	Explanatory variables
	Accommodation Services (B_AS) Population Density (S_PD) Nighttime Light Intensity (S_NTL)

Appendix C. Methodological details on explanatory variable construction using FDA-RF and SDA-RF

This research compares the methodological differences in explanatory variable construction between SDA-RF and FDA-RF. When constructing explanatory variables by FDA-RF, raster data with different resolutions were first resampled uniformly to 30 m, and 3,193,368 sampling points were generated based on the 30 m × 30 m grid. The resampled raster data were extracted according to these sampling points to generate the attribute table. Because the spatial resolution of the nighttime lighting data is 130 m, resampling it to 30 m may introduce interpolation errors or pseudo-details; therefore, this study opts to collect raw data using a 30-m grid point system. Then, based on Table C.1, the buffer generation scheme was selected and calculated to obtain the first dimension variables. For example, we created a 700 m buffer for the third category of variables based on the park AOI, from which the explanatory variables were derived by averaging the raster values within the defined buffer area (excluding those inside the park). This buffer distance was determined by setting a walking time threshold of 15 min, taking into account the non-linear characteristics of the road network, and by applying a non-linear coefficient (ranging from 1.2 to 1.4) to convert the actual walking path distance (approximately 900 m) into a straight-line distance (Lin-Chuan et al., 2016).

In the variable generation phase of SDA-RF, variables are generated according to Table C.1. For the three variables in the first class, there is no need to construct buffers during data processing; the original attribute data are used directly for analysis. For second-class variables, pixel values within the park's AOI are selected to calculate 11 probability parameters, ranging from 0 to 1 in 0.1 increments, resulting in 55 second dimension variables. For third-class variables, pixel values around the park's AOI are incorporated into the calculation. Specifically, 20 search ranges from 0.1 km to 2 km, in 0.1 km increments, are set around each park AOI. Then, 11 probability parameters, ranging from 0 to 1 in 0.1 steps, are computed, yielding 2,860 second dimension variables. A total of 2918 variables were generated during the stage.

Table C.1
The comparison of variable generation in SDA-RF and FDA-RF models.

	FDA	SDA
First-class variables	Direct use.	
Second-class variables	The pixel values within the park's AOI are averaged.	Use probability parameters to generate variables within the AOI of the park.
Third-class variables	The pixel values within the 700 m exterior buffer of the park's AOI are averaged.	Use searching ranges and probability parameters to generate second dimension variables based on the 700 m exterior buffer of the park.

Appendix D. Detailed analysis of identified zero and near-zero variance variables

Fig. D.1a shows that the proportion of zero-variance second dimension variables increases with the expansion of searching ranges, although the total number of zero and near-zero variance variables remains relatively stable. This stability is also reflected in the counts across b, where the combined number stays within a narrow range (approximately 14–16), while the composition shifts: zero-variance variables increase from 6 to 7 at $b = 0.1$–0.5 to 10–11 at $b \geq 1.1$, and near-zero variance variables decrease from 7 to 8 to 3–4. Since second dimension variables are based on buffer-scale quantile statistics, smaller searching ranges retain local geographic variation, resulting in near-zero variance. As buffer size increases, spatial homogeneity across samples rises, leading to a higher proportion of zero-variance cases. These findings highlight the high sensitivity of the second dimension variables to buffer scale, emphasizing the need for careful parameter selection based on spatial heterogeneity to avoid information redundancy and loss of predictive power.

Fig. D.1b illustrates that intermediate τ values best capture local variance among parks, while both low and high extremes result in limited differentiation across them. When $\tau = 0$, a total of 54 variables exhibit zero or near-zero variance. This is mainly because $\tau = 0$ extracts the minimum value within the buffer, and for some variables (e.g., B_BH), these minima are often identical across different sampling locations due to limited spatial variation, resulting in low variance. As τ gradually increases to 0.5, the feature values across sampling areas at the same quantile level become increasingly dispersed, and small local variances begin to emerge, causing the total number of variables to decline and eventually stabilize at around 20.

Fig. D.1c illustrates the variance distribution of variables, whose variance structure is primarily determined by their spatial resolution and sensitivity to environmental heterogeneity. Compared with other variables, the total number for B_D-1H is as high as 124, where the percentage of zero variance is 16.1%, considerably lower than for B_RND (86.4%). This is mainly because the B_D-1H data were graded into several time periods (e.g., 0–5, 5–10, 15–30 min.), and tend to yield similar accessibility values across parks within the same interval. However, the spatial resolution of B_D-1H is higher (10 m), leading to the capture of subtle differences under certain buffer and quantile combinations, so the zero-variance ratio is not as high as that of B_RND (100 m resolution). Notably, B_W-7H is calculated in a similar way to B_D—1H, but walking accessibility is more sensitive to terrain and road details and has a larger time horizon (0–420 min), thus preserving more heterogeneity around different parks and not show zero variance. Other variables such as B_BH also showed a high frequency of zero variance (90), mainly because the building heights around the parks were mostly 0 m or evenly distributed overall, which ultimately resulted in a relatively low level of variance.

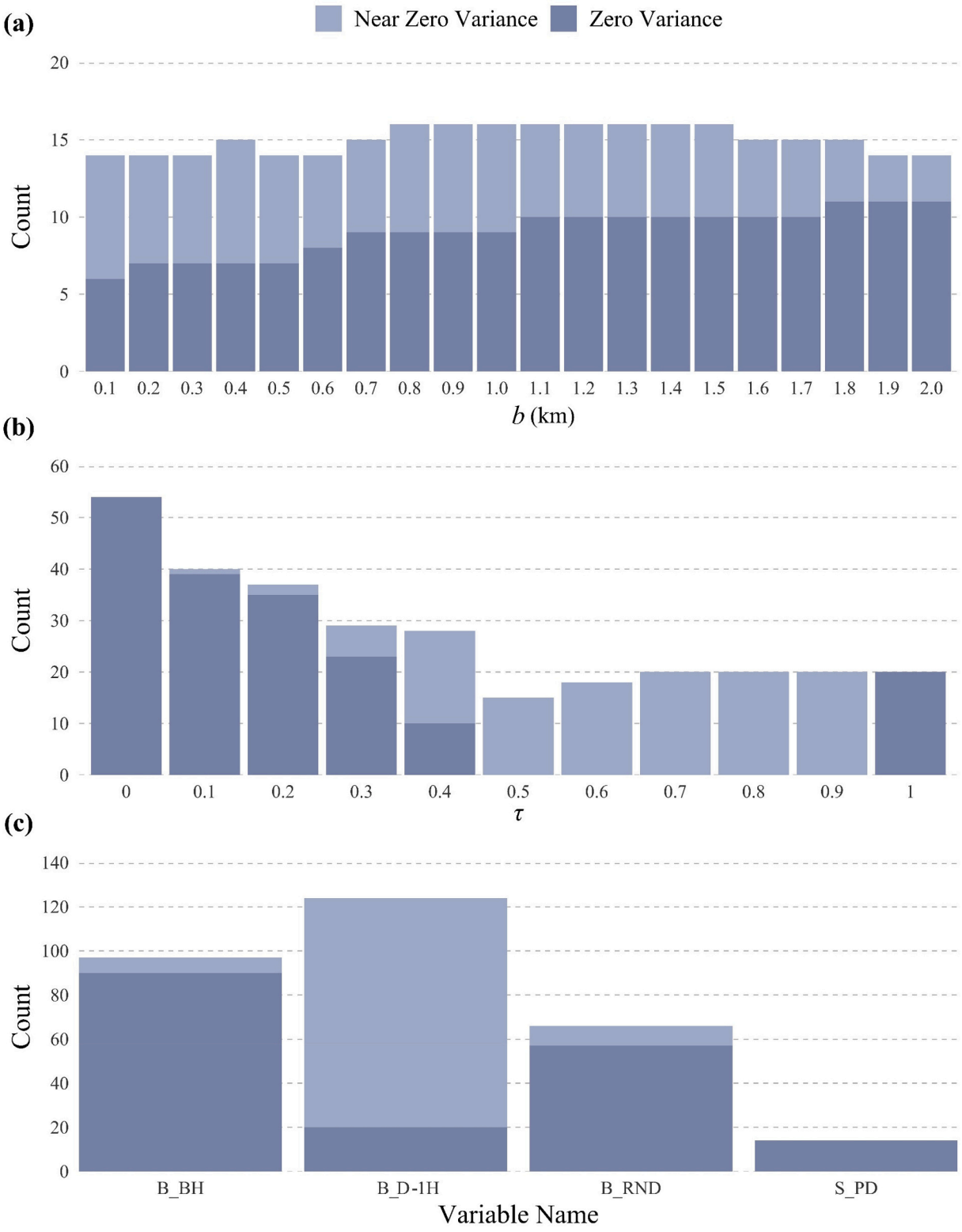

Fig. D.1. Distribution characteristics of second dimension variables identified as zero or near-zero variance features and removed during the variable screening stage. Subfigures (a), (b), and (c) respectively show the counts of such second dimension variables, summarized by searching range (b), probability parameter (τ), and variable types.

Data availability

Data will be made available on request.

References

Anselin, L. (1988). *Spatial econometrics: Methods and models* (Vol. 4). Springer Netherlands. https://doi.org/10.1007/978-94-015-7799-1

Breiman, L. (2001). Random forests. *Machine Learning, 45*(1), 5–32. https://doi.org/10.1023/A:1010933404324

Brunsdon, C., Fotheringham, A. S., & Charlton, M. E. (1996). Geographically Weighted Regression: A Method for Exploring Spatial Nonstationarity. *Geographical Analysis, 28*(4), 281–298. https://doi.org/10.1111/j.1538-4632.1996.tb00936.x

C, S. K., & RamaSree, R. J. (2015). Dimensionality reduction in automated evaluation of descriptive answers through zero variance, near zero variance and non frequent words techniques—A comparison. In *2015 IEEE 9th international conference on intelligent systems and control (ISCO)* (pp. 1–6). https://doi.org/10.1109/ISCO.2015.7282351

Chen, Y., Xu, C., Ge, Y., Zhang, X., & Zhou, Y. (2024). *A 100-m gridded population dataset of China's seventh census using ensemble learning and geospatial big data (version dataset) [dataset]*. Figshare. https://doi.org/10.6084/m9.figshare.24916140.v1

Cheng, H., Garrick, D. J., & Fernando, R. L. (2017). Efficient strategies for leave-one-out cross validation for genomic best linear unbiased prediction. *Journal of Animal Science and Biotechnology, 8*(1), 38. https://doi.org/10.1186/s40104-017-0164-6

Chiesura, A. (2004). The role of urban parks for the sustainable city. *Landscape and Urban Planning, 68*(1), 129–138. https://doi.org/10.1016/j.landurbplan.2003.08.003

Chung, W. K., Lin, M., Chau, C. K., Masullo, M., Pascale, A., Leung, T. M., & Xu, M. (2022). On the study of the psychological effects of blocked views on dwellers in high dense urban environments. *Landscape and Urban Planning, 221*, Article 104379. https://doi.org/10.1016/j.landurbplan.2022.104379

Efron, B. (1982, January). *The jackknife, the bootstrap and other resampling plans*. https://doi.org/10.1137/1.9781611970319

Engelniederhammer, A., Papastefanou, G., & Xiang, L. (2019). Crowding density in urban environment and its effects on emotional responding of pedestrians: Using wearable device technology with sensors capturing proximity and psychophysiological emotion responses while walking in the street. *Journal of Human Behavior in the Social Environment, 29*(5), 630–646. https://doi.org/10.1080/10911359.2019.1579149

Fan, Z., Duan, J., Lu, Y., Zou, W., & Lan, W. (2021). A geographical detector study on factors influencing urban park use in Nanjing, China. *Urban Forestry & Urban Greening, 59*, Article 126996. https://doi.org/10.1016/j.ufug.2021.126996

Farkas, J. Z., Hoyk, E., de Morais, M. B., & Csomos, G. (2023). A systematic review of urban green space research over the last 30 years: A bibliometric analysis. *Heliyon, 9*(2), Article e13406. https://doi.org/10.1016/j.heliyon.2023.e13406

Fotheringham, A. S., Yang, W., & Kang, W. (2017). Multiscale Geographically Weighted Regression (MGWR). *Annals of the American Association of Geographers, 107*(6), 1247–1265. https://doi.org/10.1080/24694452.2017.1352480

Gaston, K. J., Gaston, S., Bennie, J., & Hopkins, J. (2015). Benefits and costs of artificial nighttime lighting of the environment. *Environmental Reviews, 23*(1), 14–23. https://doi.org/10.1139/er-2014-0041

Ghahramani, M., Galle, N. J., Ratti, C., & Pilla, F. (2021). Tales of a city: Sentiment analysis of urban green space in Dublin. *Cities, 119*, Article 103395. https://doi.org/10.1016/j.cities.2021.103395

Grahn, P., & Stigsdotter, U. K. (2010). The relation between perceived sensory dimensions of urban green space and stress restoration. *Landscape and Urban Planning, 94*(3), 264–275. https://doi.org/10.1016/j.landurbplan.2009.10.012

Hastie, T., & Tibshirani, R. (1986). Generalized additive models. *Statistical Science, 1*(3), 297–310. https://doi.org/10.1214/ss/1177013604

Hastie, T., Tibshirani, R., & Friedman, J. (2009). *The elements of statistical learning*. Springer. https://doi.org/10.1007/978-0-387-84858-7

Hjetland, G. J., Finseråas, T. R., Sivertsen, B., Colman, I., Hella, R. T., & Skogen, J. C. (2022). Focus on self-presentation on social media across sociodemographic variables, lifestyles, and personalities: A cross-sectional study. *International Journal of Environmental Research and Public Health, 19*(17), Article 11133. https://doi.org/10.3390/ijerph191711133

Holland, J. D., & Yang, S. (2016). Multi-scale studies and the ecological neighborhood. *Current Landscape Ecology Reports, 1*(4), 135–145. https://doi.org/10.1007/s40823-016-0015-8

Hong, J., Shen, Q., & Zhang, L. (2014). How do built-environment factors affect travel behavior? A spatial analysis at different geographic scales. *Transportation, 41*(3), 419–440.

Huai, S., Liu, S., Zheng, T., & Van de Voorde, T. (2023). Are social media data and survey data consistent in measuring park visitation, park satisfaction, and their influencing factors? A case study in Shanghai. *Urban Forestry & Urban Greening, 81*, Article 127869. https://doi.org/10.1016/j.ufug.2023.127869

Huai, S., & Van de Voorde, T. (2022). Which environmental features contribute to positive and negative perceptions of urban parks? A cross-cultural comparison using online reviews and Natural Language Processing methods. *Landscape and Urban Planning, 218*, Article 104307. https://doi.org/10.1016/j.landurbplan.2021.104307

Jacobs, J. (1992). *The death and life of great American cities*. Knopf Doubleday Publishing Group.

Jiang, B. (2015). Geospatial analysis requires a different way of thinking: The problem of spatial heterogeneity. *GeoJournal, 80*(1), 1–13. https://doi.org/10.1007/s10708-014-9537-y

Juarez, P. D., Hood, D. B., Song, M.-A., & Ramesh, A. (2020). Use of an exposome approach to understand the effects of exposures from the natural, built, and social environments on cardio-vascular disease onset, progression, and outcomes. *Frontiers in Public Health, 8*, 379. https://doi.org/10.3389/fpubh.2020.00379

Kabisch, N., Qureshi, S., & Haase, D. (2015). Human–environment interactions in urban green spaces—A systematic review of contemporary issues and prospects for future research. *Environmental Impact Assessment Review, 50*, 25–34. https://doi.org/10.1016/j.eiar.2014.08.007

Kong, L., Liu, Z., Pan, X., Wang, Y., Guo, X., & Wu, J. (2022). How do different types and landscape attributes of urban parks affect visitors? Positive emotions? *Landscape and Urban Planning, 226*, Article 104482. https://doi.org/10.1016/j.landurbplan.2022.104482

Kuhn, M. (2008). Building predictive models in R using the caret package. *Journal of Statistical Software, 28*, 1–26. https://doi.org/10.18637/jss.v028.i05

Kwan, M.-P. (2012). The uncertain geographic context problem. *Annals of the Association of American Geographers, 102*(5), 958–968. https://doi.org/10.1080/00045608.2012.687349

Lai, S., Zhu, Y., & Deal, B. (2023). Did COVID-19 reshape visitor preferences in urban parks? Investigating influences on sentiments in Shanghai, China. *Sustainability, 15*(23), Article 16396. https://doi.org/10.3390/su152316396

Lapuschkin, S., Wäldchen, S., Binder, A., Montavon, G., Samek, W., & Müller, K.-R. (2019). Unmasking Clever Hans predictors and assessing what machines really learn. *Nature Communications, 10*(1), 1096. https://doi.org/10.1038/s41467-019-08987-4

Lee, J. (2011). Quality of life and semipublic spaces in high-rise mixed-use housing complexes in South Korea. *Journal of Asian Architecture and Building Engineering, 10*, 149–156. https://doi.org/10.3130/jaabe.10.149

Li, J., Fu, J., Gao, J., Zhou, R., Wang, K., & Zhou, K. (2023). Effects of the spatial patterns of urban parks on public satisfaction: Evidence from Shanghai, China. *Landscape Ecology, 38*(5), 1265–1277. https://doi.org/10.1007/s10980-023-01615-z

Li, J., Fu, J., Gao, J., Zhou, R., Zhao, Z., Yang, P., & Yi, Y. (2025). How do urban green space attributes affect visitation and satisfaction? An empirical study based on multisource data. *Cities, 156*, Article 105543. https://doi.org/10.1016/j.cities.2024.105543

Liang, H., Yan, Q., Yan, Y., Zhang, L., & Zhang, Q. (2022). Spatiotemporal study of park sentiments at metropolitan scale using multiple social media data. *Land, 11*(9), 1497. https://doi.org/10.3390/land11091497

Lin, T.-P., Matzarakis, A., & Hwang, R.-L. (2010). Shading effect on long-term outdoor thermal comfort. *Building and Environment, 45*(1), 213–221. https://doi.org/10.1016/j.buildenv.2009.06.002

Lin-Chuan, Y., Xian-Chun, Z., Shi-Jian, H., Hao-Tao, L. I. N., & Geng, C. (2016). The impact of walking accessibility of public services on housing prices: Based on the cumulative opportunities measure. *South China Journal of Economics, 34*(1), 57–70.

Lindal, P. J., & Hartig, T. (2013). Architectural variation, building height, and the restorative quality of urban residential streetscapes. *Journal of Environmental Psychology, 33*, 26–36. https://doi.org/10.1016/j.jenvp.2012.09.003

Liu, J., Dietz, T., Carpenter, S. R., Alberti, M., Folke, C., Moran, E., … Taylor, W. W. (2007). Complexity of coupled human and natural systems. *Science, 317*(5844), 1513–1516. https://doi.org/10.1126/science.1144004

Liu, Y., He, J., Wang, R., & Li, Z. (2023). The impact of urban green space on mental wellbeing: Research progress and recommendations. *Tropical Geography, 43*(9), 1747–1759. https://doi.org/10.13284/j.cnki.rddl.003733

Liu, Y., Ott, M., Goyal, N., Du, J., Joshi, M., Chen, D., … Stoyanov, V. (2019). *RoBERTa: A robustly optimized BERT pretraining approach (No. arXiv:1907.11692)*. arXiv. http://arxiv.org/abs/1907.11692.

Lundberg, S., & Lee, S.-I. (2017). *A unified approach to interpreting model predictions (No. arXiv:1705.07874)*. arXiv. https://doi.org/10.48550/arXiv.1705.07874

Ma, K., & Jiang, B. (2023). Voice of urban park visitors: Exploring destination attributes influencing behavioural intentions through online review mining. *Complex & Intelligent Systems, 9*(3), 2571–2583. https://doi.org/10.1007/s40747-020-00223-7

Ministry of Housing and Urban-Rural Development of the People"s Republic of China. (2017). *Urban Green Space Classification Standards (No. CJJ/T85-2017)*.

Nordh, H., Hartig, T., Hagerhall, C. M., & Fry, G. (2009). Components of small urban parks that predict the possibility for restoration. *Urban Forestry & Urban Greening, 8*(4), 225–235. https://doi.org/10.1016/j.ufug.2009.06.003

Payne, S. R. (2008). Are perceived soundscapes within urban parks restorative. *The Journal of the Acoustical Society of America, 123*(5_Supplement), 3809. https://doi.org/10.1121/1.2935525

Shang, Z., Cheng, K., Jian, Y., & Wang, Z. (2023). Comparison and applicability study of analysis methods for social media text data: Taking perception of urban parks in Beijing as an example. *Landscape Architecture Frontiers, 11*(5), Article 5. https://doi.org/10.15302/J-LAF-1-020083

Shao, Z., & Er, M. J. (2016). Efficient leave-one-out cross-validation-based regularized extreme learning machine. *Neurocomputing, 194*, 260–270. https://doi.org/10.1016/j.neucom.2016.02.058

Song, Y. (2022). The second dimension of spatial association. *International Journal of Applied Earth Observation and Geoinformation, 111*, Article 102834. https://doi.org/10.1016/j.jag.2022.102834

Stone, M. (1974). Cross-validatory choice and assessment of statistical predictions. *Journal of the Royal Statistical Society: Series B: Methodological, 36*(2), 111–133. https://doi.org/10.1111/j.2517-6161.1974.tb00994.x

Teng, J., Zhang, C., Gong, H., & Liu, C. (2024). Machine learning-based urban noise appropriateness evaluation method and driving factor analysis. *PLoS One, 19*(12), Article e0311571. https://doi.org/10.1371/journal.pone.0311571

UNEP (Ed.). (2019). *Global environment outlook – GEO-6: Healthy planet, healthy people* (1st ed.). Cambridge University Press. https://doi.org/10.1017/9781108627146.

Wang, J., & Xu, C. (2017). Geodetector: Principle and prospective. *Acta Geographica Sinica, 72*(1), Article 1. https://doi.org/10.11821/dlxb201701010

Widener, M. J., & Li, W. (2014). Using geolocated Twitter data to monitor the prevalence of healthy and unhealthy food references across the US. *Applied Geography, 54*, 189–197. https://doi.org/10.1016/j.apgeog.2014.07.017

Wu, W. (2022). A first Chinese building height at 10 m resolution (CNBH-10 m) [dataset]. In , *Vol. 291. Remote sensing of environment (version dataset)* (p. 113578). Zenodo. https://doi.org/10.5281/zenodo.7064268.

Xiamen Municipal Bureau of Statistics, & National Bureau of Statistics Xiamen Survey Team. (2024). *Xiamen Statistical Communiqué on National Economic and Social*

Development 2023. Xiamen Municipal Bureau of Statistics. https://tjj.xm.gov.cn/tjzl/ndgb/202403/t20240320_2829912.htm.

Xiamen Municipal People''s Government. (2013). *Notice on printing and distributing the technical regulations for urban planning management in Xiamen*. Xiamen Municipal People's Government. https://www.xm.gov.cn/zwgk/flfg/sfwj/201301/t20130104_606109.htm.

Zarghami, E., Karimimoshaver, M., Ghanbaran, A., & SaadatiVaghar, P. (2019). Assessing the oppressive impact of the form of tall buildings on citizens: Height, width, and height-to-width ratio. *Environmental Impact Assessment Review, 79*, Article 106287. https://doi.org/10.1016/j.eiar.2019.106287

Zhang, B., Xiong, W., Ma, M., Wang, M., Wang, D., Huang, X., Yu, L., Zhang, Q., Lu, H., Hong, D., Yu, F., Wang, Z., Wang, J., Li, X., Gong, P., & Huang, X. (2022). Super-resolution reconstruction of a 3 arc-second global DEM dataset. *Science Bulletin, 67* (24), 2526–2530. https://doi.org/10.1016/j.scib.2022.11.021

Zhang, J., Ma, X., Zhang, J., Sun, D., Zhou, X., Mi, C., & Wen, H. (2023). Insights into geospatial heterogeneity of landslide susceptibility based on the SHAP-XGBoost model. *Journal of Environmental Management, 336*, Article 117357. https://doi.org/10.1016/j.jenvman.2023.117357

Zhang, L., & Tan, P. Y. (2019). Associations between urban green spaces and health are dependent on the analytical scale and how urban green spaces are measured. *International Journal of Environmental Research and Public Health, 16*(4), 578. https://doi.org/10.3390/ijerph16040578

Zhang, X., & LeCun, Y. (2017). *Which encoding is the best for text classification in Chinese, English, Japanese and Korean? (No. arXiv:1708.02657)*. arXiv. https://doi.org/10.48550/arXiv.1708.02657

Zhang, Z., Yan, C., Krebs, C. J., & Stenseth, N. C. (2015). Ecological non-monotonicity and its effects on complexity and stability of populations, communities and ecosystems. *Ecological Modelling, 312*, 374–384. https://doi.org/10.1016/j.ecolmodel.2015.06.004

Zhao, T., Mu, X., & Song, W. (2023). *30-m/15-day fractional vegetation cover datasets in China (2010-2022)*. National Tibetan Plateau / Third Pole Environment Data Center. https://doi.org/10.11888/Terre.tpdc.300963

Zhao, Z., Chen, H., Zhang, J., Zhao, X., Liu, T., Lu, W., … Du, X. (2019). *UER: An open-source toolkit for pre-training models (No. arXiv:1909.05658)*. arXiv. https://doi.org/10.48550/arXiv.1909.05658

Zhao, Z., He, Q., Zhang, Y., Liu, S., & Yang, Y. (2025). Assessing cross cultural urban park emotional wellbeing impact in Shanghai and London. *Scientific Reports, 15*(1), Article 18892. https://doi.org/10.1038/s41598-025-03599-z

Zhu, Y., & Chen, Y. (2023). A study of noise exposure of traffic-type pocket parks in old urban districts based on audio-visual interaction. *Applied Acoustics, 213*, Article 109628. https://doi.org/10.1016/j.apacoust.2023.109628